Highlights

Mating versus alternative blood sources as determinants to mosquito abundance and population resilience

Gideon A. Ngwa, Bime M. Ghakanyuy, Miranda I. Teboh-Ewungkem, Jacek Banasiak

- A model for mosquito population dynamics incorporating hosts seeking and mating
- Bi-stability: Simultaneous locally stable non-zero and zero equilibria.
- Allee effect: Extinction or persistence linked to size of initial densities
- Pathway to evaluate the use of the sterile insect technique for mosquito control.

Mating versus alternative blood sources as determinants to mosquito abundance and population resilience

Gideon A. Ngwa[a,c,f], Bime M. Ghakanyuy[e,c], Miranda I. Teboh-Ewungkem[b], Jacek Banasiak[c,d]

[a] *Applied Mathematical and Computer Assisted Modelling Unit, Department of Mathematics, University of Buea, Cameroon.,*
[b] *US Department of Defense, Government, Forte Meade, MD, USA.,*
[c] *Department of Mathematics and Applied Mathematics, University of Pretoria, South Africa.,*
[d] *Institute of Mathematics, Łódź University of Technology, Łódź, Poland, Poland.,*
[e] *Department of Mathematics and Computer Science, The University of Bamenda, Bamenda, Cameroon.,*
[f] *Corresponding author: gideon.ngwa@ubuea.cm*

Abstract

A deterministic nonlinear ordinary differential equation model for mosquito dynamics in which the mosquitoes can quest for blood either within a human population or within non-human/vertebrate populations is derived and studied. The model captures both the mosquito's aquatic and terrestrial forms and includes a mechanism to investigate the impact of mating on mosquito dynamics. The model uses a restricted form of homogeneous mixing based on the idea that the mosquito has a blood-feeding habit determined by its blood-feeding preferences and its gonotrophic cycle. This characterisation allows us to compartmentalise the total mosquito population into distinct compartments according to the spatial location of the mosquito (breeding site, resting places and questing places) as well as blood-fed status. Issues of overcrowding and intraspecific competition both within the aquatic and the terrestrial stages of the mosquito's life forms are addressed and considered in the model. Results show that the inclusion of mating induces bistability, a phenomenon whereby locally stable trivial and non-trivial equilibria co-exist with an unstable non-zero equilibrium. The local nature of the stable equilibria is demonstrated by numerically showing that the long-term state of the system is sensitive to initial conditions. The bistability state is analogous to the phenomenon of the Allee effect that has been reported in population biology. The model's results, including the derivation of the threshold parameter of the system, are comprehensively tested via numerical simulations. The output of our model has direct application to mosquito control strategies, for it clearly shows key points in the mosquito's developmental pathway that can be targeted for control purposes.

Keywords: Mating, blood-feeding preferences, questing places, Allee effect

1. Introduction and background

Mosquito-borne and other indirectly transmitted diseases of humans still pose a significant challenge to global health, necessitating the need for a continued search for effective strategies to control the populations of these disease-transmitting vectors. For a mosquito-borne malaria parasite to be transmitted from one human to another human, a mosquito must (i) pick up the infection by biting an infected person, (ii) nurture and harbour the growth and maturation of the ingested parasite within its gut, (iii) transfer the now matured parasite into the bloodstream of another person at the second blood meal. So, at the centre of any mosquito-borne disease transmission is the blood-sucking mosquito. Consequently, any effective control of mosquito-borne diseases such as malaria must involve vector control, that is, management of the densities of the mosquitoes that are responsible for the transmission of the disease.

In this paper, we consider a compartmental model for the dynamics of mosquito populations. In the construction of the model, we use the fact that a mosquito needs blood for the maturation of its eggs and that the mosquito's eggs, once oviposited, require a suitable aquatic environment for their growth and development. Building the model, we take into account the fact that the mosquito undergoes complete metamorphosis and reproduces through repeated gonotrophic cycles. Thus, the densities of the different life forms of the mosquitoes: aquatic juvenile forms in an aquatic environment, adult mosquitoes at the breeding sites, adult mosquitoes at questing places (which include human and non-human habitat sites), and adult mosquitoes at resting places (where fully blood-fed adults rest before returning to the breeding site to lay eggs) are the main state variables in the model. The compartmentalisation also divides the mosquito population into male and female groups and further subdivides the female population into sub-classes representing their blood meal status (fully blood-fed or questing for blood), their blood preference (zoophilic or anthropophilic) and physiological status (mated or not mated). Thus, our model considers often neglected realistic factors such as mosquitoes' blood meal preferences. In fact, we are proposing an alternative way of thinking about the mosquito-borne disease control problem by focusing on the mosquitoes that carry the parasites from human to human. Previous models have not fully captured these aspects. For example, the model proposed in [26] and also in [3, 4] divides the mosquito populations into male and female without considering their blood meal status and preference factors, while the model proposed in [32] and further studied in [33] takes into account the different blood meal status of the mosquitoes without, however, subdividing the mosquito population into male and female or accounting for the population of mosquitoes that fed from nonhuman sources. These are crucial factors in the mosquito's life and should be considered when building a model to understand the dynamics of the mosquito population.

Hence, the main objective of this paper is to present a comprehensive ordinary differential equation model that captures the above-mentioned stages of the mosquito life cycle. We study how mosquitoes in these different stages are integrated into a single dynamical system, mathematically capturing the interactions between mosquitoes themselves and the blood hosts to model the dynamics of their populations.

The rest of the paper is organised as follows. In Section 2, we present a derivation of the mathematical model, including the model's variables and schematics, discuss the types of mating encounters, examine choices of appropriate oviposition functions, and present properties of the model, including issues of existence and stability of steady-state solutions. Numerical simulations in Section 3 demonstrate our model's different stability properties. In Section 4, we study the effect of mating and alternative blood sources on our model's output by examining different sub-models that capture different combinations of questing formats and mating proper. We round up the paper with a discussion and conclusions in Section 5. The proofs of mathematical results and other technicalities required in the paper are discussed in the Appendices A & B.

2. Model Derivation, Basic Properties and Analysis

In this section, we develop a compartmental system modelling the flow between the compartments and changes within them by nonlinear ordinary differential equations.

2.1. Description of the Model

In Table 1, we list the state variables in the model, and in Table 2, we list the parameters used in the model. The flow chart illustrating the compartments and the links between them is shown in Figure 1.

State Variables	**Description of Variables**	**Quasi-dimension**
A	Density of aquatic lifeforms.	A_q
F_B	Density of unfertilized female mosquitoes emerging from the aquatic stage at the breeding site.	M
M_B	Density of male mosquitoes emerging from the aquatic stage at the breeding site at the breeding site.	M
B	Density of fertilised female mosquitoes at the breeding site.	M
Q_H	Density of fertilised female mosquitoes questing blood from humans.	M
Q_V	Density of fertilized female mosquitoes questing blood from nonhuman vertebrates.	M
R_V	Density of mosquitoes that fed from a nonhuman vertebrate and are resting before returning to the breeding site and laying eggs there at a rate λ.	M
R_H	Density of mosquitoes that fed from humans and are resting before returning to the breeding site and laying eggs there at a rate λ.	M
H	Constant human population density.	H
V	Constant vertebrate population density.	V

Table 1: Description of state variables showing their quasi-dimension. In the quasi-dimension, A_q represents aquatic density, M mosquito density, H human density and V vertebrate density.

Parameter	Description of Parameters	Quasi-dimension	Parameter value\ Range	Reference
θ	Proportion of aquatic forms that develop into unfertilized female mosquitoes; $1-\theta$ is the proportion developing into males.	1	0.5	[37]
θ_1	Fraction of female mosquitoes fertilized after mating.	1	$0-1$	
γ	Rate at which aquatic forms transition into terrestrial forms.	T^{-1}	$\frac{1}{14}-\frac{1}{7}day^{-1}$	[17]
ξ	Bio-transition factor from aquatic biomass into terrestrial forms density.	MA_q^{-1}		
μ_y	Natural death rate of the mosquitoes of type y, where y denotes one of the adult mosquito-types.	T^{-1}	Males: $\frac{1}{7}-\frac{1}{6}\ day^{-1}$, Females: $\frac{1}{28}-\frac{1}{14}\ day^{-1}$	[42]
$a_V,\ a_H$	Rates at which reproductive female mosquitoes return to the breeding site from vertebrate, a_V, respectively, human, a_H, habitats, to lay eggs.	T^{-1}	$0.1-1\ day^{-1}$	[12, 32]
λ_0	Limiting number of aquatic life forms generated by type R mosquitoes when population numbers are extremely small. This quantity is weighted by the function $\tilde{\lambda}(R)$ to produce the oviposition function $\lambda(R)=\lambda_0\tilde{\lambda}(R)$	A_qM^{-1}	Bifurcation parameter	
κ	Rate at which mosquitoes leave the breeding site to quest for blood.	T^{-1}	$0.1-0.5\ day^{-1}$	[16, 46]
ω_V	The nonhuman vertebrate blood preference factor.	MV^{-1}	$\omega_V=0.5\omega_H$ so that $\varsigma=\frac{\omega_V}{\omega_H}=0.5\ HV^{-1}$	Estimated
ω_H	The human blood preference factor.	MH^{-1}	$\omega_H=2\omega_V$	Estimated
τ_V	Effective mass action contact parameter between zoophilic mosquitoes and vertebrates.	$V^{-1}T^{-1}$	$0.4\ V^{-1}day^{-1}$	Estimated
τ_H	Effective mass action contact parameter between anthropophilic mosquitoes and humans.	$H^{-1}T^{-1}$	$0.2\ H^{-1}day^{-1}$	Estimated
p,q	Probabilities that a mosquito successfully harvests a blood meal from a human (p) or vertebrate (q) populations, $0\leq p,q\leq 1$.	1	$0.70-0.95$	[13, 32]
μ_{A1}	Natural death rate of aquatic life forms.	T^{-1}	$0.05-0.15$	[8, 16]
μ_{A2}	Additional death of aquatic forms due to overcrowding	$A_q^{-1}T^{-1}$	$0.001-0.01\ A_q^{-1}day^{-1}$	[8, 16]
S	Constant mass action contact parameter between female and male mosquitoes.	$M^{-1}T^{-1}$	$0.01\ M^{-1}day^{-1}$	Estimated
L_P	Carrying capacity of the pond.	A_q	$1000\ A_q$	Estimated
L	Carrying capacity of the breeding site.	M	$100\ M$	Estimated

Table 2: Table of parameters, their descriptions and quasi-dimensional units. In addition to the quasi-dimensional units explained in Table 1, T represents time and 1 identifies a dimensionless parameter.

The stages of life of mosquitoes are divided into two broad groups based on their living environment: the aquatic and the terrestrial. The aquatic stage comprises the juvenile forms (egg, larva, pupa) that eventually develop into terrestrial forms (the adult mosquitoes). We shall represent the aquatic forms of the mosquito with the state variable A. The terrestrial mosquitoes are further compartmentalised according to their physiological and blood preference status. We have (i) newly emerged adult female and male mosquitoes that are swarming at the breeding site to mate, represented by F_B and M_B, (ii) newly and previously fertilized females that have returned to the breeding site to lay eggs, denoted by B, (iii) questing mosquitoes (that is, mosquitoes seeking for blood within human and nonhuman vertebrate populations), which we represent by Q, and (iv) blood-fed mosquitoes that are resting before returning to the breeding site to lay eggs, denoted by R. Since we are accounting for both human and nonhuman blood sources, the questing mosquitoes, and hence fed and resting mosquitoes, can be in one of two sub-compartments depending on their blood source: those that quest and successfully feed on humans will be identified by the subscript H and those that quest and successfully feed on nonhumans will be identified by the subscript V.

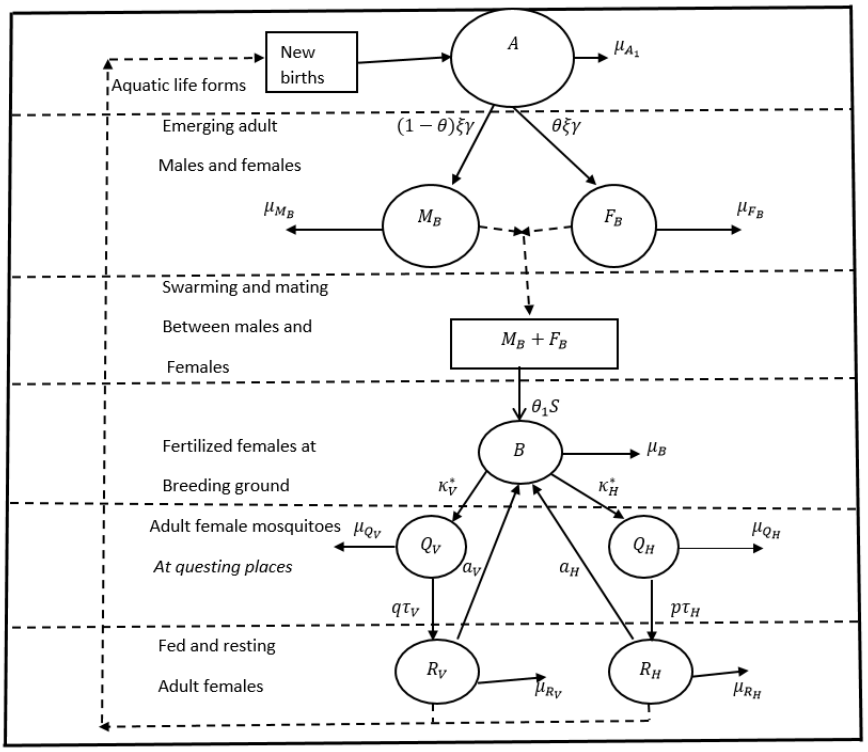

Figure 1: A flowchart showing the life and reproduction stages of mosquitoes and their progression from one stage to the other, which are described in detail in this section. The notation was introduced in Tables 1 and 2.

We can consider the life cycle of mosquitoes beginning with adult mosquitoes ovipositing eggs into an aquatic environment. The eggs eventually develop into adult mosquitoes according to a maturation process that follows their metamorphic developmental pathway, involving the aquatic and terrestrial life stages. The adult mosquitoes start their terrestrial life either as males or females. The total population density of all newly emerged adult mosquitoes, at any time t, is $F_B(t) + M_B(t)$. These mosquitoes are available to take part in the mating process. We denote by γ the rate at which the aquatic biomass is depleted by the emergence of the terrestrial forms and set ξ to be a parameter describing the transition factor from the biomass into the terrestrial individual mosquitoes. A proportion θ of the emerging juvenile mosquitoes will develop into females, while $1 - \theta$ gives the proportion that will become males.

Newly emerged mosquitoes congregate in swarms near their breeding ground, and mating ensues [43]. We assume all newly emerged female mosquitoes are unfertilized and only unfer-

tilized females mate. Further, as in [35], each unfertilized female mosquito mates only once. We shall view mating as the outcome of an interactive encounter between male and female mosquitoes through the lens of incidence rates.

Once a female mosquito is fertilised, it seeks to ingest blood needed for the maturation of its eggs. The source of blood will depend on the blood preference factor of the mosquito. Some species of mosquitoes prefer human blood (anthropophilic), while others prefer nonhuman vertebrate blood (zoophilic). So, the decision to visit a human or a nonhuman environment for a blood meal will be determined by the blood preference index of a particular mosquito, as well as the availability of a host. As described above, we will identify mosquitoes that feed on humans by the subscript H and those that feed on vertebrates by the subscript V. Thus, when fertilised mosquitoes, B, leave the breeding site to quest for a blood meal, they become questing mosquitoes Q; specifically, Q_H quest within a human population and Q_V quest within nonhuman populations. The questing mosquitoes may acquire a blood meal to become fed and resting mosquitoes, denoted by R_H if the blood source was human and R_V otherwise. Only fully blood-fed and resting vectors can lay eggs upon return to a breeding site. These eggs will hatch to continue the mosquito's life cycle.

2.2. Mating, Oviposition and Recruitment Rates

Here, we present a brief discussion on the mating, recruitment, flow and exposure rates within the mosquito populations, and between the mosquito, humans and non-human vertebrate populations.

1. *Mating*: While there are many ways to capture mosquito-mosquito interaction, here we borrow from the idea of incidence rates in disease modelling. If we let ϱ be the average number of male mating encounters per unit time, then M_B male mosquitoes will make ϱM_B such encounters per unit time. Then, ϱM_B is adjusted with $\frac{F_B}{F_B+M_B}$, the chance of finding a female unfertilised mosquito, to get $\varrho\frac{F_B}{F_B+M_B}M_B$ fertilisation encounters per unit time. This is the *standard incidence rate* formulation; [36]. In another formulation, we can use the law of mass action from chemical kinetics; [30], by considering the reaction sequence $F_B + M_B \xrightarrow{S} \Gamma + M$. For a justification of using the mass action law in insect mating, we refer the reader to, e.g., [40]. Here, we interpret the process by saying that females interact with males at a rate S, resulting in female fertilisation. Thus, $\Gamma = SF_BM_B$ is the rate of total fertilisation of females, which then appear in B, setting the stage for their questing. In all cases, only a fraction of the encounters will lead to proper fertilisation. For mathematical tractability, in this article, we shall use mass action to model the mating encounters. It is important to note the following:
   (a) During mating, mosquitoes can become more vulnerable to predators as the act of mating itself is energy intensive and can distract them, making them easier targets for predators, see [1], [11].
   (b) A successful mating occurred when a female was fertilised and successfully exited the mating site.

   So, only a fraction of mated female mosquitoes continue as fertilised females.
2. *Oviposition or recruitment into aquatic stages*: The oviposition or recruitment function into the aquatic form is a key determinant of the size of the newly emerged adult mosquito population and, thus, the eventual adult mosquito eclosion rate. Under ideal conditions (ideal temperature, appropriate precipitation, availability of an ideal breeding site, available blood sources), the relationship between the aquatic life forms and the ovipositing adult types is approximately linear. However, any deviations from the ideal circumstances will change the form of the relationship, which becomes non-linear. The capacity of an average pond at the breeding site to receive and sustain oviposited eggs can also be a

limiting factor. Additionally, the net recruitment rate into the aquatic life stage will also be determined by the fecundity of the blood-fed females, as well as by the rate at which these rested females return to the breeding site and can lay eggs. This suggests that the recruitment rate into the aquatic stages will no longer be a linear function of the resting mosquito population $R = R_V + R_H$. It is, therefore, necessary to consider a suitable non-linear recruitment function to model the oviposition. Suppose a blood-fed and resting mosquito lays $\lambda(R)$ eggs (treated as aquatic biomass) per mosquito of each type in one cycle, where $\lambda : [0, \infty) \to \mathbb{R}$ is a non-increasing, continuously differentiable function, which is nonnegative on the range of R. Then, R mosquitoes will lay $R\lambda(R)$ eggs in the aquatic environment. So anthropophilic mosquitoes will lay $R_H\lambda(R)$ eggs, and the zoophilic ones $R_V\lambda(R)$. Thus, the recruitment rate, Γ_R, into the aquatic stage, initialised by the laying of eggs, is given by

$$\Gamma_R(R) = a_H R_H \lambda(R) + a_V R_V \lambda(R), \tag{1}$$

where a_H and a_V are the respective rates at which anthropophilic and zoophilic mosquitoes return from their resting places to the breeding sites to lay eggs. Various forms of the recruitment function, λ, with the desired properties (real-valued, continuously differentiable, monotonic non-increasing), have been proposed and explained in the literature. These include a constant function, logistic, Ricker, and Maynard-Smith-Slatkin recruitment functions[1]. See for example [18, 31, 34, 33, 47].

2.3. Model Equations

In this section, we present the equations that describe the dynamics within the aquatic and adult mosquito classes, starting with the aquatic stages.

Aquatic stages (A): The density of aquatic lifeforms, A, increases when fed and resting female mosquitoes return and lay eggs via the oviposition function $\lambda(R)$, leading to creation of new aquatic forms at the rate $\Gamma_R(R)$ derived in (1). The density of aquatic lifeforms is reduced due to natural death and overcrowding (due to the limited capacity of ponds supporting the aquatic lifeforms), and when aquatic lifeforms successfully transform into terrestrial mosquitoes at the rate γ per the aquatic life form.

The aquatic environment can be a collection of ponds and puddles or a large reservoir of standing water. For the purpose of this work, we shall assume that the breeding site is a collection of ponds, where each pond is assumed to have a finite carrying capacity, indicating the amount of aquatic life forms that each pond can sustain. We expect the carrying capacity of the entire breeding site (the entire aquatic environment) to be the sum of the carrying capacities of the individual ponds. Let L_P be the total carrying capacity of the environment and let $A(t)$ denote the density of aquatic lifeforms there at any time t. Then $1 - \frac{A(t)}{L_P}$ is the fraction of aquatic lifeforms that can still be added into the pond. Thus, the equation modelling A takes the form:

$$\frac{dA}{dt} = (a_H R_H + a_V R_V) \cdot \lambda(R) \cdot \left(1 - \frac{A}{L_P}\right) - (\gamma + \mu_{A1} + \mu_{A2} A)\, A, \tag{2}$$

where γ, L_P, α, a_H, μ_{A1}, μ_{A2}, and a_V are positive constants described in Tables 2.

Terrestrial stages of the mosquitoes: Aquatic forms of the insect develop via the metamorphic developmental pathway to become adults, differentiating into either males or females. We do not address the issue of sex ratio in the current modelling framework, however, some

[1]For a constant recruitment function, $R\lambda(R) = \lambda_0 R$ for some constant λ_0, while for a Ricker function, it takes the form $R\lambda(R) = \tilde{\lambda}_* R e^{-R/\tilde{L}}$, and for a Maynard-Smith-Slatkin, the form is $R\lambda(R) = \frac{\tilde{\lambda}_* R}{1+\left(\frac{R}{\tilde{L}}\right)^n}$.

studies indicate that developing mosquito juveniles tend to exhibit bias towards more males than females, while others point to an equal proportion of males and females being produced at certain times of the day, [28]. Here, we assume that a fraction θ of the developing juveniles mature to become female mosquitoes while the remaining proportion $1-\theta$ of aquatic forms will develop into males. That is, we recognise that different fractions can develop into male and female mosquitoes as follows:

Male mosquitoes M_B: The density of the male mosquitoes increases when a proportion, $1-\theta$ of aquatic lifeforms successfully develop at the rate $\xi\gamma$ into adult male mosquitoes, where ξ is the bio-transition factor measuring the successful transition from aquatic life forms into adults that are terrestrial life forms, and decreases as a result of natural death at the rate μ_{M_B}. Here, we do not consider other forms of death. Thus, the equation governing the density of male mosquitoes is

$$\frac{dM_B}{dt} = (1-\theta)\xi\gamma A - \mu_{M_B} M_B. \tag{3}$$

The unfertilized female mosquitoes F_B: The density of unfertilized females increases when aquatic lifeforms develop into adult female mosquitoes and decreases due to natural death per female mosquito but also when mating results in fertilization (modelled here via mass action contact). We assume that a fraction θ_1 of female mosquitoes are successfully fertilized after mating encounter, while the remaining $1-\theta_1$ are assumed to die. We interpret the case $\theta_1 = 1$ as perfect mating so efficient that all female mosquitoes are fertilized during mating. The equation for the density of the unfertilized female mosquitoes is thus given by:

$$\frac{dF_B}{dt} = \theta\xi\gamma A - SF_B M_B - \mu_{F_B} F_B, \tag{4}$$

where $SF_B M_B$ is interpreted as $\theta_1 SF_B M_B + (1-\theta_1) SF_B M_B$; compare with (7). All parameters are as earlier defined in Tables 2.

The fertilized breeding site mosquitoes B: The density of type B mosquitoes increases when a fraction, θ_1, of unfertilized females becomes fertilized after mating with mass action contact parameter S, and when previously fertilized, fed and reproducing mosquitoes of type R_V and R_H return from resting places to the breeding site at rates a_V and a_H, respectively. The density of class B decreases at the rate μ_B per B mosquito due to natural death and when they leave the breeding site to quest for blood.

Flow rate of fertilized mosquitoes to questing places: We assume that humans, H, and other vertebrates, V, reside at separate spatial locations, called the human and vertebrate sites, or habitats. These habitats are referred to as *questing places*. In this paper, we assume that H and V are constant, indicating thus an abundant presence of blood sources for the mosquito. Let ω_V and ω_H denote, respectively, the number of mosquitoes per non-human and human that prefer the respective blood source. Then a total of $\omega_V V$ mosquitoes prefer questing for blood from non-humans, while $\omega_H H$ will quest human blood and $\frac{\omega_V V}{\omega_V V+\omega_H H}$, respectively, $\frac{\omega_H H}{\omega_V V+\omega_H H}$, are the proportion of meals from non-humans and humans. In extreme cases, when $\omega_H = 0$ or $H = 0$, we have exclusive questing within non-human or animal populations, and when $\omega_V = 0$ or $V = 0$, the mosquitoes quest exclusively in human populations. Since we are mostly interested in the human-mosquito interaction and its link to disease transmission dynamics, we shall assume that $\omega_H > 0$ and define $\varsigma = \frac{\omega_V}{\omega_H} \geq 0$. Then,

$$\text{Mosquitoes questing in human habitats} = \frac{\omega_H H}{\omega_V V + \omega_H H} B = \frac{H}{\varsigma V + H} B \tag{5}$$

$$\text{Mosquitoes questing in non-human habitats} = \frac{\omega_V V}{\omega_V V + \omega_H H} B = \frac{\varsigma V}{\varsigma V + H} B. \tag{6}$$

If $0 \leq \varsigma < 1$, then more female mosquitoes quest within human populations (that is, we have a larger proportion of anthropophilic female mosquitoes), and if $\varsigma > 1$, then we have a larger proportion of zoophilic mosquitoes). If $\varsigma = 1$, only the respective sizes of V and H will determine the proportions in the flow to different questing places. Nonetheless, even if ς is small, the size of ςV could be of relative significance depending on the size of V. The question of strict blood preference for mosquitoes has not been addressed in this model, but the emphasis is on questing places. If κ is the rate at which mosquitoes leave the breeding sites, then (5) and (6) yield

$$\begin{aligned}\frac{dB}{dt} &= \theta_1 S M_B F_B + a_V R_V + a_H R_H - \kappa\left(\frac{H}{H+\varsigma V}\right)B - \kappa\left(\frac{\varsigma V}{H+\varsigma V}\right)B - \mu_B B \\ &= \theta_1 S M_B F_B + a_V R_V + a_H R_H - \kappa B - \mu_B B,\end{aligned} \tag{7}$$

where all parameters found in this equation are as defined in Table 2.

The questing mosquitoes: When fertilised mosquitoes arrive at questing places in search of a blood meal, they change status to become questing-type, Q, mosquitoes, divided into Q_H mosquitoes seeking human blood and Q_V mosquitoes seeking non-human blood. We assume that there is a cost to questing as follows: (i) mosquitoes questing for human blood can either succeed in drawing blood with probability p or fail with probability $1-p$, (ii) mosquitoes questing for non-human blood succeed with probability q and fail with probability $1-q$. It is assumed that any failure at questing leads to the death of the questing mosquito. We assume that $0 \leq p \leq q \leq 1$ since humans are more capable of protecting themselves from being bitten. If p and q are both very small, then this assumption translates into the fact that many mosquitoes will die during questing. In the case where blood sources are protected, by, say, insecticide-impregnated screens, this may be reasonable. This is, however, unlikely in nature. The phenomenon of multiple feeding attempts by questing mosquitoes, whereby some questing mosquitoes that failed to take a full blood meal during a blood questing episode are allowed to try questing again, has been examined in [18]. It is shown there that allowing the mosquito multiple feeding opportunities increases the survival chances of the insect. Here, for simplicity and mathematical tractability, we continue to impose this high cost of questing, but assume not too small values of p and q, in the model since the focus of this current paper is to investigate the effects of mating and alternative blood sources on the population resilience. Once mosquitoes succeed in drawing blood, they change status and become fed and resting type mosquitoes, R_H if they fed on human blood and R_V otherwise. Additionally, questing mosquitoes die naturally at their respective rates μ_{Q_V} and μ_{Q_H} per mosquito. Thus, the equations for the population densities of questing female mosquitoes are

$$\frac{dQ_H}{dt} = \kappa\left(\frac{H}{H+\varsigma V}\right)B - \mu_{Q_H} Q_H - (1-p)\tau_H H Q_H - p\tau_H H Q_H, \tag{8}$$

$$\frac{dQ_V}{dt} = \kappa\left(\frac{\varsigma V}{H+\varsigma V}\right)B - \mu_{Q_V} Q_V - (1-q)\tau_V V Q_V - q\tau_V V Q_V. \tag{9}$$

Fed and resting mosquitoes: The densities of R_H and R_V, defined above, decrease by natural death with rates, respectively, μ_H and μ_V, and when they leave to return to the breeding site to lay eggs, at the rates a_H and a_V defined above. Thus,

$$\frac{dR_H}{dt} = p\tau_H H Q_H - \mu_{R_H} R_H - a_H R_H, \tag{10}$$

$$\frac{dR_V}{dt} = q\tau_V V Q_V - \mu_{R_V} R_V - a_V R_V, \tag{11}$$

where all parameters are described the Tables 1 and 2. Combining equations (2)–(11), we obtain

$$\left.\begin{array}{rcl}
\frac{dA}{dt} & = & (a_H R_H + a_V R_V)\cdot\lambda(R)\cdot\left(1-\frac{A}{L_P}\right) - (\gamma+\mu_{A1}+\mu_{A2}A)\,A,\\
\frac{dM_B}{dt} & = & (1-\theta)\xi\gamma A - \mu_{M_B} M_B,\\
\frac{dF_B}{dt} & = & \theta\xi\gamma A - S M_B F_B - \mu_{F_B} F_B,\\
\frac{dB}{dt} & = & \theta_1 S M_B F_B + a_H R_H + a_V R_V - \kappa B - \mu_B B,\\
\frac{dQ_H}{dt} & = & \kappa\left(\frac{H}{H+\varsigma V}\right) B - \tau_H H Q_H - \mu_{Q_H} Q_H,\\
\frac{dQ_V}{dt} & = & \kappa\left(\frac{\varsigma V}{H+\varsigma V}\right) B - \tau_V V Q_V - \mu_{Q_V} Q_V,\\
\frac{dR_H}{dt} & = & p\tau_H H Q_H - a_H R_H - \mu_{R_H} R_H,\\
\frac{dR_V}{dt} & = & q\tau_V V Q_V - a_V R_V - \mu_{R_V} R_V,
\end{array}\right\} \tag{12}$$

where $R = R_V + R_H$. To complete the formulation of the system, we specify the initial conditions

$$\begin{array}{rcl}
A(0) & = & A_0,\ M_B(0) = M_{M0},\quad F_B(0) = F_{B0}, R_V(0) = R_{V0},\quad R_H(0) = R_{H0},\\
B(0) & = & B_0,\quad Q_V(0) = Q_{V0},\quad Q_H(0) = Q_{H0}.
\end{array} \tag{13}$$

As we shall see later, the choice of initial conditions plays an important role in the final solution.

2.3.1. Basic Properties of the Model

To describe the basic properties of the model developed here, we start by examining the total adult mosquito population. Let $N = F_B + M_B + B + Q_H + Q_V + R_H + R_V$ be the total density of terrestrial mosquitoes. Then, adding the respective equations in system (12), we get

$$\begin{array}{rcl}
\frac{dA}{dt} & = & (a_H R_H + a_V R_V)\cdot\lambda(R)\cdot\left(1-\frac{A}{L_P}\right) - (\gamma+\mu_{A1}+\mu_{A2}A)\,A \qquad (14)\\
\frac{dN}{dt} & = & \gamma\xi A - (1-p)\tau_H H Q_H - (1-q)\tau_V V Q_V - (1-\theta_1) S M_B F_B\\
 & & -(\mu_{F_B} F_B + \mu_{M_B} M_B + \mu_B B + \mu_{Q_H} Q_H + \mu_{Q_V} Q_V + \mu_{R_V} R_V + \mu_{R_H} R_H). \qquad (15)
\end{array}$$

The subsystem (14) and (15) captures the interactions between the totality of terrestrial and the aquatic forms, showing how type R mosquitoes reproduce, giving birth to aquatic forms of type A, which later mature to produce more terrestrial forms.

While under the adopted assumptions on λ, it is easy to see that (12) has unique locally defined solutions for any initial condition, a biological requirement is that for each nonnegative initial population, there is a bounded nonnegative solution that exists all the time. Here, the recruitment function λ plays a crucial role. In Proposition 2.1 we address the issue of boundedness and positivity of solutions whenever λ is nonnegative on $[0,\infty)$; a more general case is referred to Section 2.4.

Proposition 2.1. *Let $\lambda : [0, \infty) \to [0, \infty)$ be the recruitment function. If $L_P < \infty$ and the initial conditions are nonnegative with $A_0 < L_P$, or if $L_P = \infty$ and $A(t)$ is bounded, then any solution of system* (12)*, and hence of* (14) –(15)*, is nonnegative and bounded, and hence exists for all t.*

Proof. See Appendix B.1

We highlight a few advantages of the modelling framework presented here.

1. If either $\xi = 0$ or $\gamma = 0$, then $\frac{dN}{dt} < 0$ and so $N(t) \to 0$ as $t \to \infty$ so that both $R_H(t)$ and $R_V(t)$ tend to 0 as $t \to \infty$ and the mosquito population becomes eventually extinct for any initial conditions.
2. If $p = q = 0$, all questing attempts lead to the death of the mosquito, that is, all female mosquitoes die during questing. This again would lead to the extinction of the total mosquito population, since in this case, $R_H \to 0$ and $R_V \to 0$ and, finally, $A \to 0$, leading to $N \to 0$.
3. If $p = q = 1$, all questing mosquitoes succeed in blood-feeding and live to lay eggs, thereby contributing to mosquito abundance.
4. High cost of questing, that is, large mass action contact parameters τ_H and τ_V, negatively impacts the total mosquito population, as seen in the negative terms in (15).
5. If $0 \leq \theta_1 \ll 1$, almost all mating encounters lead to death, leading to the eventual extinction of the mosquito population. The parameter θ_1 can be used to assess the effectiveness of mosquito control methods via mating interruptions using, say, the sterile insect release method [5, 48, 24].
6. High cost of mating represented here in a large mass action contact parameter S has a negative impact on the total mosquito population, as seen in negative terms in Equation (15).
7. If $a_H = a_V = 0$, no blood-fed and resting mosquitoes return to a breeding site after their resting period following the blood meal and hence no eggs are laid. Consequently, $A(t) \to 0$ as $t \to \infty$, leading to the extinction of all terrestrial forms.

Several combinations of these parameters and scenarios further highlight other properties of our model. The provided list emphasizes the strength and applicability of our modelling framework by showing the main parameters where control measures can be applied. Some of the aspects have been pointed out before; see, for example, [34, 33, 32, 18]. The novelty in the current model lies in the fact that we have incorporated the idea of an alternative blood source in the dynamic, which, to the best of our knowledge, has not been fully addressed before.

2.4. On the Choice of an Appropriate Oviposition function

The oviposition, or recruitment, function λ is an important driver for the process, and we shall demonstrate below that it must remain positive for the model to yield realistic (non-negative) solutions for all time. Typical examples of such functions, reviewed in [18, 33], include:

$$\lambda_1(R) = \lambda_0 \left(1 - \frac{R}{L}\right), R \in [0, L), \quad \text{the logistic birth rate,} \tag{16}$$

$$\lambda_2(R) = \frac{\lambda_0}{1 + \left(\frac{R}{L}\right)^n}, n \geq 1, \quad \text{the Maynard–Smith–Slatkin function.} \tag{17}$$

The constant L can be arbitrarily large and is linked to the carrying capacity of the breeding site. We see that λ_2 satisfies the assumptions of Proposition 2.1. However, when using λ_1, the positivity of the solution is guaranteed only as long as we can ensure that $R(t) < L$ (note that

it is not automatic as the equation for A is not a logistic equation – the carrying capacity L does not refer to the solution A) and, as demonstrated below, λ_1 may induce negative solutions if $R(t)$ exceeds L. Despite this drawback, we shall see below that it is still an acceptable choice for an appropriate selection of parameters.

2.4.1. When is λ_1 a tenable choice?

The reason why λ_1 often appears in modelling is that it can be obtained as a linear approximation of a general decreasing function λ in a neighbourhood of some point $\tilde{R}$,

$$\lambda(R) \approx \lambda(\tilde{R}) + \lambda'(\tilde{R})(R - \tilde{R}) = \lambda_0 \left(1 - \frac{R}{L}\right),$$

where $\lambda_0 = \lambda(\tilde{R}) - \lambda'(\tilde{R})\tilde{R}$ and $L = \frac{\lambda_0}{-\lambda'(\tilde{R})}$. Such an approximation could be used if we could keep the solution close to $\tilde{R}$, which is not always feasible.

Example 2.1. *We immediately see that such a model is not well-posed in the positive orthant. Indeed, assume an empty pool of water and a large swarm of reproducing mosquitoes arriving from elsewhere. If $R > L$, then at time $t = 0$ we have*

$$\left.\frac{dA}{dt}\right|_{t=0} < 0, \quad A(0) = 0,$$

and $A(t) < 0$, at least for some $t > 0$.

However, as shown below, the solution remains in the positive orthant under certain conditions. More precisely, we shall show that if $L_p < \infty$, then for any selection of parameters and the size of the initial conditions, the solution is nonnegative if the carrying capacity L is sufficiently large. On the other hand, if $L_P = \infty$, the same result holds if a certain combination of the parameters is smaller than 1. This is achieved through a series of lemmas stated below, but whose proofs are postponed to Appendix B.

Recall that for a vector $\boldsymbol{z} = (z_1, \ldots, z_k)$, we write $\boldsymbol{z} \geq \mathbf{0}$ if all entries of $\boldsymbol{z}$ are non-negative, $\boldsymbol{z} > \mathbf{0}$ if, in addition, at least one entry is positive, and $\boldsymbol{z} \gg \mathbf{0}$ if all entries are positive. Furthermore, we denote

$$\|\boldsymbol{z}\|_1 = \sum_{i=1}^{k} z_i. \tag{18}$$

We denote

$$\boldsymbol{x}_0 = (x_{i0})_{1 \leq i \leq 8} = (A_0, M_{B0}, F_{B0}, B_0, Q_{H0}, Q_{V0}, R_{V0}, R_{H0}) \tag{19}$$

and let

$$\boldsymbol{x}(t) = \boldsymbol{x}(t, \boldsymbol{x}_0) = (x_i(t))_{1 \leq i \leq 8} = (A(t), M_B(t), F_B(t), B(t), Q_H(t), Q_V(t), R_V(t), R_H(t)) \tag{20}$$

be the solution emanating from $\boldsymbol{x}_0$.

For further use, we also introduce a subdivision of $\boldsymbol{x}$ as

$$\boldsymbol{x} = (A, \boldsymbol{J}, \boldsymbol{Y}) = (A, \boldsymbol{J}, B, \boldsymbol{Y}_Q, \boldsymbol{Y}_R),$$

where $\boldsymbol{J} := (M_B, F_B)$ are the juvenile mosquitoes and $\boldsymbol{Y} := (B, Q_H, Q_V, R_V, R_H) = (B, \boldsymbol{Y}_Q, \boldsymbol{Y}_R)$ are the mature ones, with analogous split $\boldsymbol{x}_0 = (A_0, \boldsymbol{J}_0, \boldsymbol{Y}_0) = (A_0, \boldsymbol{J}_0, B_0, \boldsymbol{Y}_{Q0}, \boldsymbol{Y}_{R0})$ for the initial conditions. First, we observe that (12) is locally well-posed in $\mathbb{R}^8$, that is, for any

$\boldsymbol{x}_0 \in \mathbb{R}^8$, there is a solution $\boldsymbol{x}(t)$ defined on a maximal forward interval of existence (depending, in general, on $\boldsymbol{x}_0$). Further, using [39, Theorem B.7], we see that if $\boldsymbol{x}_0 \geq \mathbf{0}$, then $\boldsymbol{x}(t) \geq \mathbf{0}$ as long as $(a_H R_H(t) + a_V R_V(t))\lambda(R) \geq 0$.

Lemma 2.1. *If the following conditions:*

$$(i) \quad \boldsymbol{x}_0 > \mathbf{0}, \tag{21a}$$

$$(ii) \quad If\ A_0 = 0\ and\ \boldsymbol{Y}_0 = \mathbf{0},\ then\ \boldsymbol{J}_0 \gg 0, \tag{21b}$$

$$(iii) \quad R_0 = R_{H0} + R_{V0} < L, \tag{21c}$$

are satisfied, then there is $\delta > 0$ such that $\boldsymbol{x}(t) \gg \mathbf{0}$ on $(0, \delta)$.

Proof. See Appendix B.2

Remark 2.1. *If in Lemma 2.1, in the assumption* (21b) $\boldsymbol{J}_0 \gg 0$ *was replaced by either $M_{B0} > 0$ and $F_{B0} = 0$, or conversely, then, by the uniqueness, $(0, M_{B0}e^{-t\mu_{M_B}}, 0, 0, 0, 0, 0)$ or $(0, 0, F_{B0}e^{-t\mu_{F_B}}, 0, 0, 0, 0)$, respectively, would be the only solution to* (12) *emanating from those initial conditions. So, if we remove* (21b) *from Lemma 2.1, we can only claim that $\boldsymbol{x}(t) > \mathbf{0}$ on some $(0, \delta)$.*

Lemma 2.2. *Let the conditions of Lemma 2.1 be satisfied. If $R(t_0) = 0$ and $\boldsymbol{x}(t)$ is a nonnegative solution to* (12) *for $[0, t_0]$, then there is $\delta > 0$ such that $R(t) > 0$ for $t \in (t_0, t_0 + \delta)$ and $\boldsymbol{x}(t)$ can be extended as a nonnegative solution to $[0, t_0 + \delta]$. In other words, $R(t)$ cannot leave $[0, L]$ through the left end.*

Proof. See Appendix B.3

Lemma 2.3. *Assume that there exists $A_M < \infty$ such that $A(t) \leq A_M$ for all $t \geq 0$. If $\boldsymbol{x}(t, \boldsymbol{x}_0)$ with $\boldsymbol{x}_0$ satisfying assumption (i) of Lemma 2.1 is a non-negative solution on $[0, T)$, $0 < T \leq \infty$ and*

$$\begin{aligned} L &> R_{\max}(A_M) \\ &:= \max\left\{ \|\boldsymbol{Y}_0\|_1, \frac{\theta_1 S}{\mu} M_{B0} F_{B0}, \frac{\theta_1 S}{\mu} \frac{\theta\xi\gamma}{\mu_{F_B}} M_{B0} A_M, \frac{\theta_1 S}{\mu} \frac{(1-\theta)\xi\gamma}{\mu_{M_B}} F_{B0} A_M, \frac{\theta_1 S}{\mu} \frac{\theta(1-\theta)\xi^2\gamma^2}{\mu_{F_B}\mu_{M_B}} A_M^2 \right\}, \end{aligned} \tag{22}$$

then $R(t) < L$ on $[0, T]$ and hence $\boldsymbol{x}(t, \boldsymbol{x}_0)$ is non negative on $[0, \infty)$.

Proof. See Appendix B.4

Since $\frac{dA}{dt}\big|_{A=L_P} < 0$, we immediately get

Corollary 2.1. *If the conditions of Lemma* (2.1) *are satisfied, $L_P < \infty$, $\boldsymbol{x}_0$ is such that $0 < A_0 < L_P$ and $L > R_{\max}(L_P)$, then $\boldsymbol{x}(t, \boldsymbol{x}_0)$ is a globally defined nonnegative solution to* (12).

Lemma 2.4. *Let $L_P = \infty$. Then*

$$A(t) \leq \max\left\{ A_0, \frac{\frac{\gamma+\mu_1}{\mu_2} + \sqrt{\left(\frac{\gamma+\mu_1}{\mu_2}\right)^2 + \frac{\max\{a_V, a_H\}\lambda_0 L}{\mu_2}}}{2} \right\} \tag{23}$$

as long as $0 \leq R(t) \leq L$.

Proof. See Appendix B.5

Corollary 2.2. *Assume that the assumptions of Lemma* (2.1) *is satisfied,* $L_P = \infty$ *and*

$$\frac{\theta_1 S\theta(1-\theta)\xi^2\gamma^2\lambda_0 \max\{a_H, a_V\}}{\mu_{F_B}\mu_{M_B}\mu\mu_2} < 1 \tag{24}$$

and L *is sufficiently large, then* $\boldsymbol{x}(t)$ *is a globally defined nonnegative solution to* (12).

Proof. See Appendix B.6

To summarise, the above analysis shows that subject to certain restrictions on the parameters, the logistic oviposition function 16 is still useful. In fact, any oviposition function that becomes negative for large R negative will have analogous restrictions on the parameters and constraints. It is, therefore, appropriate to retain only those oviposition functions that are positive for all values of R, such as (17). That the Maynard–Smith–Slatkin oviposition function is more suitable for modelling mosquito dynamics was observed already in [33]. Thus, we shall use the logistic oviposition function only for comparison purposes and mathematical illustrations.

2.5. Nondimensionalisation and Reparameterisation

To scale the system, we consider the following change of variables (see Appendix A):

$$\left.\begin{array}{rcl}
t &=& \frac{t^*}{a_H+\mu_{R_H}}, \quad M_B = \frac{(a_H+\mu_{R_H})M_B^*}{S}, \quad A = \frac{(a_H+\mu_{R_H})\mu_{M_B}A^*}{S(1-\theta)\xi\gamma}, \\
B &=& \left(\frac{\theta}{1-\theta}\right)\left(\frac{\mu_{M_B}}{S}\right)B^*, \quad F_B = \left(\frac{\theta}{1-\theta}\right)\left(\frac{\mu_{M_B}}{S}\right)F_B^*, \\
Q_H &=& \left(\frac{\kappa_H^*}{\tau_H H+\mu_{Q_H}}\right)\left(\frac{\theta}{1-\theta}\right)\left(\frac{\mu_{M_B}}{S}\right)Q_H^*, \quad Q_V = \left(\frac{\kappa_V^*}{\tau_V V+\mu_{Q_V}}\right)\left(\frac{\theta}{1-\theta}\right)\left(\frac{\mu_{M_B}}{S}\right)Q_V^*, \\
R_H &=& p\left(\frac{\tau_H H}{\tau_H H+\mu_{Q_H}}\right)\left(\frac{\kappa_H^*}{a_H+\mu_{R_H}}\right)\left(\frac{\theta}{1-\theta}\right)\left(\frac{\mu_{M_B}}{S}\right)R_H^*, \\
R_V &=& q\left(\frac{\tau_V V}{\tau_V V+\mu_{Q_V}}\right)\left(\frac{\kappa_V^*}{a_V+\mu_{R_V}}\right)\left(\frac{\theta}{1-\theta}\right)\left(\frac{\mu_{M_B}}{S}\right)R_V^*.
\end{array}\right\} \tag{25}$$

Substituting (25) in the unscaled system (12) and then, for notational convenience, dropping the asterisks, we have the scaled system

$$\left.\begin{array}{rcl}
\frac{dA}{dt} &=& (\alpha_1 R_H + \alpha_2 R_V)\cdot\lambda\left(\eta_1 L R_H + \eta_2 L R_V\right)\cdot(1-\eta_3 A) - (\alpha_3+\alpha_4 A)\,A, \\
\frac{dM_B}{dt} &=& \beta_1\left(A - M_B\right), \\
\frac{dF_B}{dt} &=& A - M_B F_B - \beta_2 F_B, \\
\frac{dB}{dt} &=& \theta_1 M_B F_B + \delta_1 R_H + \delta_2 R_V - \beta_3 B, \\
\frac{dQ_H}{dt} &=& \rho_1\left(B - Q_H\right), \\
\frac{dQ_V}{dt} &=& \rho_2\left(B - Q_V\right), \\
\frac{dR_H}{dt} &=& Q_H - R_H, \\
\frac{dR_V}{dt} &=& \rho_3\left(Q_V - R_V\right),
\end{array}\right\} \tag{26}$$

where

$$\left.\begin{array}{rcl}
\kappa_H^* &=& \kappa\left(\frac{H}{H+\varsigma V}\right), \quad \kappa_V^* = \kappa\left(\frac{\varsigma V}{H+\varsigma V}\right), \\
\alpha_1 &=& p\left(\frac{a_H}{a_H+\mu_{R_H}}\right)\left(\frac{\tau_H H}{\tau_H H+\mu_{Q_H}}\right)\left(\frac{\kappa_H^*}{a_H+\mu_{R_H}}\right)\left(\frac{\xi\gamma\theta}{a_H+\mu_{R_H}}\right), \\
\alpha_2 &=& q\left(\frac{a_V}{a_V+\mu_{R_V}}\right)\left(\frac{\tau_V V}{\tau_V V+\mu_{Q_V}}\right)\left(\frac{\kappa_V^*}{a_H+\mu_{R_H}}\right)\left(\frac{\xi\gamma\theta}{a_H+\mu_{R_H}}\right), \\
\eta_1 &=& p\left(\frac{\tau_H H}{\tau_H H+\mu_{Q_H}}\right)\left(\frac{\kappa_H^*}{a_H+\mu_{R_H}}\right)\left(\frac{\theta}{1-\theta}\right)\left(\frac{\mu_{M_B}}{LS}\right), \\
\eta_2 &=& q\left(\frac{\tau_V V}{\tau_V V+\mu_{Q_V}}\right)\left(\frac{\kappa_V^*}{a_V+\mu_{R_V}}\right)\left(\frac{\theta}{1-\theta}\right)\left(\frac{\mu_{M_B}}{LS}\right), \\
\eta_3 &=& \frac{(a_H+\mu_{R_H})\mu_{M_B}}{L_P S(1-\theta)\xi\gamma}, \quad \alpha_3 = \frac{\gamma+\mu_{A1}}{a_H+\mu_{R_H}} \quad \alpha_4 = \frac{\mu_{M_B}\mu_{A2}}{S(1-\theta)\xi\gamma}, \\
\beta_1 &=& \frac{\mu_{M_B}}{a_H+\mu_{R_H}}, \quad \beta_2 = \frac{\mu_{F_B}}{a_H+\mu_{R_H}}, \quad \beta_3 = \frac{\kappa+\mu_B}{a_H+\mu_{R_H}}, \\
\delta_1 &=& p\left(\frac{\tau_H H}{\tau_H H+\mu_{Q_H}}\right)\left(\frac{a_H}{a_H+\mu_{R_H}}\right)\left(\frac{\kappa_H^*}{a_H+\mu_{R_H}}\right), \\
\delta_2 &=& q\left(\frac{\tau_V V}{\tau_V V+\mu_{Q_V}}\right)\left(\frac{a_V}{a_V+\mu_{R_V}}\right)\left(\frac{\kappa_V^*}{a_H+\mu_{R_H}}\right), \\
\rho_1 &=& \frac{\tau_H H+\mu_{Q_H}}{a_H+\mu_{R_H}}, \quad \rho_2 = \frac{\tau_V V+\mu_{Q_V}}{a_H+\mu_{R_H}}, \quad \rho_3 = \frac{a_V+\mu_{R_V}}{a_H+\mu_{R_H}}.
\end{array}\right\} \tag{27}$$

In Remark 2.2 below, we assess the relative sizes of the scaled parameters.

Remark 2.2 (On the relative sizes of the scaled parameters.). *We can make the following remarks about the parameter groupings:*

1. *The parameter κ measures the flow rate from the breeding site to questing places while the parameters a_H and a_V both measure the flow rate from the resting places to the breeding site. It is reasonable to assume that the resting places are nearer the breeding site so that $\kappa \leq \max\{a_H, a_V\}$. So, assume that $\kappa_H^* \leq a_H$ and $\kappa_V^* \leq a_V$.*
2. *We can write $\alpha_1 = \epsilon_p \frac{\kappa_H^* \xi\gamma}{a_H}$ with $\epsilon_p \in [0,1]$. Similarly, we can write $\alpha_2 = \epsilon_q \frac{\kappa_V^* \xi\gamma}{a_v}$ with some $\epsilon_q \in [0,1]$, the scaled parameter. So, the size of $\xi\gamma$ is the main driver of these parameters.*
3. *Similarly, we see that the parameters $\eta_1, \eta_2, \eta_3, \alpha_3, \alpha_4$, are positive.*
4. *It has been reported that female mosquitoes, on average, live longer than their corresponding male mosquitoes [14, 19, 44]. Also, emerging mosquitoes try to mate quickly, so the duration of the juvenile stage is shorter than the life span of the adult ones, leading to $0 < \beta_2 \leq \beta_1 < 1$. That is, the unfertilized females are at most as old as the males, and $0 < \beta_3 < 1$. From the forgoing discussion about κ and a_H, $0 < \delta_1, \delta_2 < 1$.*
5. *From the description, we have $0 < \rho_1, \rho_2, \rho_3 < \infty$.*
6. *Since $\delta_1 < \frac{\kappa_H^*}{a_H+\mu_{R_H}}$ and $\delta_2 < \frac{\kappa_V^*}{a_H+\mu_{R_H}}$, we have that $\delta_1 + \delta_2 < \frac{\kappa_H^*+\kappa_V^*}{a_H+\mu_{R_H}} = \frac{\kappa}{a_H+\mu_{R_H}} < \frac{\kappa+\mu_B}{a_H+\mu_{R_H}} = \beta_3$, and so by transitivity, $\delta_1 + \delta_2 < \beta_3$.*

2.6. Scaled Model: Existence and Stability of Steady State Solutions

Let, as before, $\boldsymbol{x} : [0,\infty) \to \mathbb{R}^8$ be a column vector of state variables in $\mathbb{R}^8$, defined in (20). Let $\boldsymbol{f} : \mathbb{R}^8 \to \mathbb{R}^8$, $\boldsymbol{f} : \boldsymbol{x} \mapsto (f_1(\boldsymbol{x}), f_2(\boldsymbol{x}), \cdots, f_8(\boldsymbol{x}))$, be a vector of functions on the right-hand side of (26) so that the system can be written compactly in the form

$$\frac{d\boldsymbol{x}}{dt} = \boldsymbol{f}(\boldsymbol{x}), \quad \boldsymbol{x}(0) = \boldsymbol{x}_0, \tag{28}$$

where $\boldsymbol{x}(0)$ is given by (19). As noted above, if λ is differentiable, then $\boldsymbol{f} \in \mathcal{C}^1(\mathbb{R}^8; \mathbb{R}^8)$ and hence for any $\boldsymbol{x}_0 \in \overline{\mathbb{R}}^8_+$, there exists a unique local solution $\boldsymbol{x}(t) \in \mathbb{R}^8_+$. If $\lambda(R)$ is nonnegative for all $R \geq 0$ or, for logistic λ, additionally the assumptions of Section 2.4 are satisfied, then this solution is nonnegative and exists for all $t > 0$. Hence, our system is well-posed from a mathematical and biological standpoint.

2.6.1. Existence of Realistic Steady State Solutions

The class of solutions we are interested in are *steady state* or *stationary solutions* and their stability. We are only concerned with realistic solutions in the sense of Definition 2.1.

Definition 2.1 (Realistic solution.). *A solution $\boldsymbol{x}$ of* (28)*, where the detailed form of $\boldsymbol{f}$ is given by* (26)*, is called realistic if all its components are non-negative.*

Theorem 2.1 (Existence of Steady State Solutions.). *System* (28) *possesses a trivial steady state $E_0^* = \mathbf{0} = (0,0,0,0,0,0,0,0)$, which always exists for all parameter regimes. Furthermore, any non-trivial steady state $E_P^* = \boldsymbol{x}^* = (A^*, M_B^*, F_B^*, B^*, Q_H^*, Q_V^*, R_H^*, R_V^*)$ satisfies*

$$B^* = Q_H^* = Q_V^* = R_H^* = R_V^*, A^* = M_B^*, F_B^* = \frac{A^*}{A^* + \beta_2} = \frac{M_B^*}{M_B^* + \beta_2}, \tag{29}$$

together with the two equations

$$\left.\begin{array}{ll} (i) & R_H^* = c\frac{A^{*2}}{A^*+\beta_2}, \\ (ii) & \lambda\left(LR_H^*(\eta_1+\eta_2)\right) = \frac{(\alpha_3+\alpha_4 A^*)(A^*+\beta_2)}{bA^*(1-\eta_3 A^*)} =: g(A^*), \end{array}\right\} \tag{30}$$

where

$$c = \frac{\theta_1}{\beta_3 - \delta_1 - \delta_2} > 0, \qquad b = (\alpha_1 + \alpha_2)c > 0. \tag{31}$$

Proof. See Appendix B.7

Function g, as constructed in (30), plays an important role in the forthcoming analysis. We summarize its properties in the following lemma.

Lemma 2.5. *The g is positive on the interval $(0, \eta_3^{-1})$ and has a single minimum at $A_m^* \in (0, \eta_3^{-1})$. Furthermore, g is strictly decreasing on the interval $(0, A_m^*)$, and strictly increasing on the interval (A_m^*, η_3^{-1}) with $\lim_{A\to 0+} g(A) = \lim_{A\to \frac{1}{\eta_3}-} g(A) = +\infty$. Also, g is strictly concave upwards.*

Proof. See Appendix B.8

As we noted above, if $A(0) > \frac{1}{\eta_3}$ and $\lambda(R) \geq 0$ for all $R \geq 0$, $\frac{dA}{dt} < 0$, that is $A(t)$ decreases as t increases. Thus, to fix attention, will consider $0 \leq A(t) \leq \frac{1}{\eta_3}$.

Before formulating the next theorem, we observe that if $A^* = 0$, then from (30) and (29), all the other components of the equilibrium are zero, and we have the trivial steady state E_0^*. On the other hand, $A^* = \frac{1}{\eta_3}$ is not a valid steady state solution because, referring to (30) and (29), that will be possible only in the biologically unrealistic case $(\alpha_3 + \frac{\alpha_4}{\eta_3})\frac{1}{\eta_3} = 0$.

Theorem 2.2 (On the existence of a non-trivial equilibrium.). *Assume that λ is a strictly decreasing function. There exists a threshold parameter $\mathcal{B}_\lambda$ such that $\mathcal{B}_\lambda > 1$ is a necessary condition for the steady state system* (30) *and* (29) *to have at least one non-trivial solution with $A^* \in (0, \frac{1}{\eta_3})$ and there is only trivial solution if $\mathcal{B}_\lambda \leq 1$.*

Proof. See Appendix B.9

A more precise description of the structure of equilibria and a better estimate of the threshold can be obtained if we specify the oviposition function.

Remark 2.3. *If we consider $\lambda = \lambda_0 = const$, then an argument analogous to that in the proof of Theorem 2.2 shows that if $\mathcal{B}_\lambda > 1$, then there are exactly two positive solutions, if $\mathcal{B}_\lambda = 1$, then there is one positive solution and there are no positive solutions if $\mathcal{B}_\lambda < 1$, see [7]. Hence, in this case, $\mathcal{B}_\lambda$ is the genuine threshold.*

Theorem 2.3. *Let the oviposition function λ_2 be the Maynard Smith-Slatkin function, defined in* (17)*, with $n = 1$. There is a unique threshold $b^*\lambda_0^* > \alpha_4\beta_2 + \alpha_3$ such that there are no positive steady states if $b\lambda_0 < b^*\lambda_0^*$, a unique positive steady state if $b\lambda_0 = b^*\lambda_0^*$ and two positive steady states if $b\lambda_0 > b^*\lambda_0^*$. Any positive steady state, whenever exists, satisfies $A^* \in \left(0, \frac{1}{\eta_3}\right)$. Moreover, if $A_1^*(b\lambda_0) < A_2^*(b\lambda_0)$ are two steady states, then, monotonically,*

$$\lim_{b\lambda_0\to\infty} A_1^*(b\lambda_0) = 0, \quad \lim_{b\lambda_0\to\infty} A_2^*(b\lambda_0) = \eta_3^{-1}. \tag{32}$$

Proof. See Appendix B.10

Remark 2.4. *We observe that the threshold $\mathcal{B}_{\lambda_2}$, corresponding to general $\mathcal{B}_\lambda$, that is, such that if $\mathcal{B}_{\lambda_2} \leq 1$ precludes the existence of positive equilibria, is given here by*

$$\mathcal{B}_{\lambda_2} = \frac{b\lambda_0}{\alpha_3 + \beta_2\alpha_4} > \mathcal{B}_\lambda,$$

where we used $\nu > \alpha_4\beta_2$.

For numerical purposes, we can provide a better estimate of the threshold $\lambda_0^* b^*$. Indeed, from the proof, we see that

$$z_{min} \leq z^* \leq \bar{z},$$

where $\bar{z}$ is the positive solution to

$$\psi(z) = a_2^2 z^2 - 18a_3a_2a_0z - 27a_3^2a_0^2 - 4a_2^3a_0 = 0.$$

The second inequality follows from the fact that, by the definition, $\Psi(z) > \psi(z)$ for $z > 0$. Then, solving the quadratic equations,

$$\alpha_3+\alpha_4\beta_2+\frac{\sqrt{a_2^4 + 216a_3^2a_2a_0} - a_2^4}{12a_3} < \lambda_0^*b^* < \alpha_3+\alpha_4\beta_2+\frac{18a_3a_0+\sqrt{18^2a_3^2a_2^2a_0^2 + 4(27a_3^2a_0^2 + 4a_2^3a_0)}}{2a_2}$$

Theorem 2.4. *Let the oviposition function be the logistic function, defined in* (16) *and satisfying assumptions introduced in Section 2.4. There exists a unique threshold value $\lambda_0^*b^*$, such that there are no solutions for $\lambda_0 b < \lambda_0^*b^*$, exactly one solution for $\lambda_0 b = \lambda_0^*b^*$ and two solutions for $\lambda_0 b > \lambda_0^*b^*$, in $(0, \eta_3^{-1})$. Moreover, if $A_1^*(\lambda_0 b) < A_2^*(\lambda_0 b)$ are the two positive steady states, then, monotonically*

$$\lim_{\lambda_0 b\to\infty} A_1^*(\lambda_0 b) = 0, \quad \lim_{\lambda_0 b\to\infty} A_2^*(\lambda_0 b) = x^*, \tag{33}$$

where

$$x^* = \begin{cases} \eta_3^{-1} & \text{if } A_+ \geq \eta_3, \\ A_+ & \text{if } A_+ < \eta_3, \end{cases}$$

and $A_+ = \frac{1+\sqrt{1+4\sigma\beta_2}}{2}$.

Proof. See Appendix B.11

In what follows, we assume that the oviposition function is either the logistic λ_1, (16) with assumptions of Section 2.4, or the Maynard Smith–Slatkin λ_2, (17) with $n = 1$, function and hence the statements of Theorems 2.3 and 2.4 hold.

Theorem 2.5. *The stability of the trivial steady state is determined by the roots of the 5th degree polynomial:*

$$P_5(\zeta) = (-\zeta - \rho_2)(-\zeta - \rho_3)(\delta_1\rho_1 - (\zeta + 1)(\beta_3 + \zeta)(\zeta + \rho_1)) + \delta_2\rho_2\rho_3(\zeta + 1)(\zeta + \rho_1). \tag{34}$$

Proof. See Appendix B.12

A preliminary criterion for the stability of DFE can be obtained using the Gershgorin theorem, [21]. For a better understanding of the conditions, we use here the parameters of the original system (12).

Proposition 2.2. *If*

$$\mu_{A1} > (\xi - 1)\gamma, \quad \mu_{R_H} > a_H\lambda_0, \quad \mu_{R_V} > a_V\lambda_0, \tag{35}$$

then the trivial equilibrium of (12) *is asymptotically stable.*

Proof. See Appendix B.13

Corollary 2.3. *Suppose* $\rho_1 = \rho_2$, $\rho_3 = 1$. *Then the trivial steady state is always locally asymptotically stable.*

Proof. See Appendix B.14

Remark 2.5. *To explain the meaning of the assumptions* $\rho_1 = \rho_2$, $\rho_3 = 1$ *in Corollary 2.3, we refer to* (27) *and observe that then*

1. *the rates at which reproductive female adult mosquitoes return to the breeding sites from questing places,* a_V *and* a_H *are equal,*
2. *the natural death rate is the same for all classes of mosquitoes,*
3. *the mass action parameters* $\tau_H H$ *and* $\tau_V V$ *are the same.*

Though these assumptions, especially the third one, appear to be very restrictive, they offer us an important glimpse into the effect of alternative blood sources in the model. As we shall see in the numerical explorations below, even without these restrictions in place, the trivial steady state is still stable for a range of parameter values, pointing out the fact that alternative blood sources may only add variety to the survivability options for the mosquitoes but do not affect the stability properties of the steady states.

2.7. The Existence of a Threshold Parameter and Bi-stability

An important outcome of our modelling is the identification of a unique threshold parameter

$$\mathcal{B} = \frac{\lambda_0 b}{\lambda_0^* b^*}, \tag{36}$$

determining the emergence of non-trivial steady states. Unfortunately, we do not have an analytic expression for the threshold, and hence, we cannot identify it with the basic offspring number for the mosquito population dynamics, at which the population can establish itself in the environment. The usual interpretation allows one to define the basic offspring number, see [34], as the average number of new adult mosquitoes that can arise from one reproducing adult mosquito during the entire period of its reproductive life. Interestingly, as we will demonstrate numerically below, for the model with mating and alternative blood sources studied here, the threshold parameter affects only the existence and size of the equilibria but does not affect their stability. That is, as we will see, the parameter $\mathcal{B}$ has the following properties: (i) when $\mathcal{B} \in [0, 1)$, the system has only the trivial steady state, which is locally asymptotically stable, (ii) when $\mathcal{B} > 1$, asymptotically stable trivial steady state co-exists with two non-trivial equilibria, one of which is always locally asymptotically stable, while the other is unstable. The simultaneous existence and stability properties of the three equilibria existing when $\mathcal{B} > 1$ is called bi-stability; this property in one-dimensional ecological models, when the middle equilibrium is unstable, is called the *Allee effect*, [2]. Here, we will see a scenario in which the

basins of attraction of the trivial and stable non-trivial equilibria are both non-empty sets that are not singletons. It is possible, therefore, to achieve extinction of the mosquito population even when $\mathcal{B} > 1$ by driving the system to the basin of attraction of the trivial equilibrium. Such a result has not been observed so far for these classes of models.

We see from (31) that the parameter b appearing in the threshold parameter $\mathcal{B}$ can be written as

$$b = c\alpha_1 + c\alpha_2 = c\frac{\xi\gamma\theta}{(a_H + \mu_{R_H})^2}\left(\frac{p\kappa_H^* a_H}{a_H + \mu_{R_H}}\frac{\tau_H H}{\tau_H H + \mu_{Q_H}} + \frac{q\kappa_V^* a_V}{a_V + \mu_{R_V}}\frac{\tau_V V}{\tau_V V + \mu_{Q_V}}\right), \qquad (37)$$

which shows that the threshold has components from the human and an alternate blood source. Recalling the definition of c in (31), $c = \frac{\theta_1}{\beta_3 - \delta_1 - \delta_2}$, we see that also the parameter θ_1 plays an important role as small θ_1, which indicates an inefficiency in mating, can drive $\mathcal{B}$ to small values, leading to eventual extinction.

Our model has thus identified several pathways to extinction. For instance, (i) we can have extinction when $\theta_1 \to 0$ because of mating inefficiencies, (ii) we can have extinction when the initial conditions of the process lie within the basin of attraction of the trivial steady state, (iii) we can have extinction when there is oviposition deficiency, that is, λ_0 is small), (iv) we can have extinction when $\xi \to 0$ or $\gamma \to 0$ (inefficient bio-transfer from aquatic to terrestrial). Note that cases (iii) and (iv) are covered by Proposition 2.2.

3. Numerical Simulations

In this section, we conduct a numerical study to better understand the stability properties of solutions of (26), useing the logistic oviposition function (16). We shall consider the following cases.

1. $0 < \mathcal{B} < 1$. For the parameters in this range, the system has only the trivial steady state. Results from numerical simulations, as reported below, suggest that when $0 < \mathcal{B} < 1$, the trivial steady state is globally asymptotically stable.
2. $\mathcal{B} > 1$. Here, we have two non-trivial steady states coexisting with the trivial steady state. The results from the numerical studies indicate that when we have three steady states corresponding to $A = A_0^* = 0, A = A_1^*, A = A_2^*$, which, for definiteness, we order as $A_1^* < A_2^*$, the steady states corresponding to $A = 0$ and $A = A_2^*$ are locally asymptotically stable while that corresponding to $A = A_1^*$ is unstable. Thus, we see the phenomenon of bi-stability. The real challenge is to determine the basins of attraction for the two attracting steady states. We demonstrate numerically that the basins of attraction for the steady states corresponding to $A^* = A_0^* = 0$ and $A^* = A_2^* > 0$ are non-empty.

In the simulations presented in Figs. 2 and 3, we use the following parameter values: $\lambda_0 = 10,\ a_H = 0.6,\ a_V = 0.3,\ L = 100, L_P = 1000,\ \gamma = 0.7,\ \mu_{A1} = 0.05,\ \theta = 0.5,\ \xi = 0.6,\ \tau_H = 0.2,\ \tau_V = 0.4,\ \mu_{Q_H} = \mu_{Q_V} = \mu_{R_H} = \mu_{R_V} = \mu_B = \mu_{F_B} = 0.04,\ \mu_{M_B} = 0.2,\ p = 0.86,\ q = 0.9, \kappa = 0.4,\ S = 0.01,\ \theta_1 = 0.8, V = 10^6,\ H = 10^4,\ \varsigma = 0.5,\ \mu_{A2} = 0.05$. With these parameter values, $\mathcal{B}_\lambda = 3.86603 > 1$, and we have three steady-state solutions: $A^* = 0, A_1^* = 0.0131388$, and $A_2^* = 2.56464$.

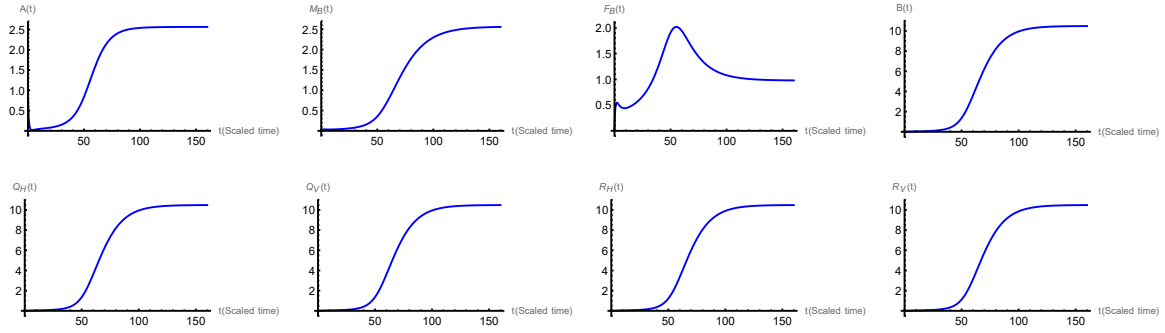

Figure 2: Numerical integration results showing the long-term solutions for all the state variables of (26). The initial data, $A(0) = 1.1$, with all other variables set at zero, are in the basin of attraction of the steady state corresponding to $A^* = 2.56464$, even though the trivial steady state is also stable.

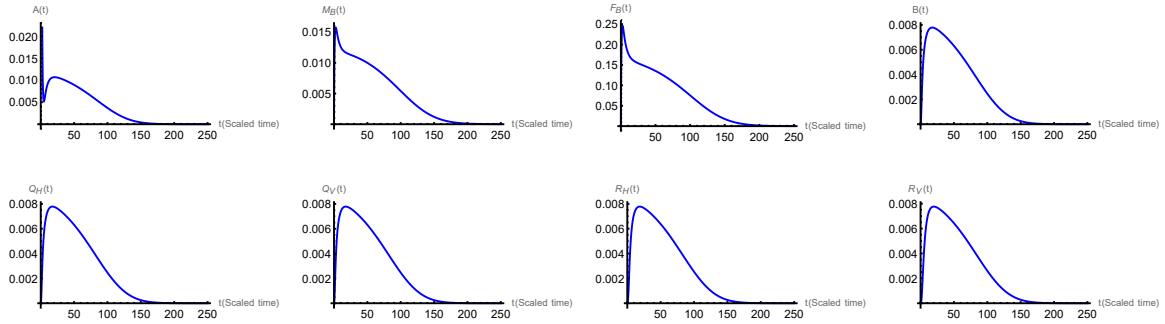

Figure 3: Numerical integration results showing the long-term behaviour of all state variables of (26). We use the same parameters as in Figure 2 but change the initial condition to $A(0) = 0.4$. As the solution profiles show, all variables decay to zero with time. Here, the initial conditions are in the basin of attraction of the trivial equilibrium, even though it co-exists with a non-trivial state.

In the next figure, maintain the same parameter values, except for the value of λ_0, which is changed from $\lambda_0 = 10$ to $\lambda_0 = 0.5$. With this change, we have $\mathcal{B}_\lambda = 0.193302 < 1$, and hence, the trivial equilibrium is unique.

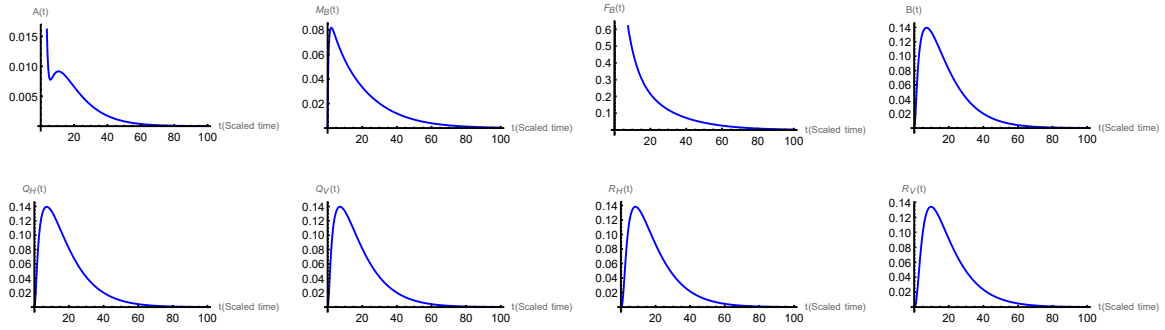

Figure 4: Numerical integration results showing the long-term solutions for all state variables of (26). The unique trivial steady state is asymptotically stable, suggesting its global stability in this case.

To better understand the dynamics of (26), we numerically investigated how the steady states of the system vary with increasing $\lambda_0 b$. Since the trivial steady state always exists, we focus only on the non-trivial steady states, and, for brevity, we will only consider varying λ_0. We observed that the threshold parameter $\mathcal{B}$ increases with λ_0 and there exists a unique value value of $\lambda_0 = \lambda_0^c$ at which $\mathcal{B} = 1$. As λ_0 further increases beyond λ_0^c, $\mathcal{B}$ increases to $\mathcal{B} > 1$, and

the analysis above shows that the system switches from having exactly one, trivial, equilibrium to having multiple equilibria.

Now, we provide a numerical illustration of the above considerations. Using the parameter values introduced before Figure 2, we vary λ_0 starting from zero and observe that, indeed, there exists a threshold value λ_0^c, such that when $\lambda_0 < \lambda_0^c$, the trivial steady state is the only steady state solution. At $\lambda_0 = \lambda_0^c$, the system experiences a saddle-node bifurcation at which a new steady state emerges, which then splits into two steady states corresponding to A_1^* and A_2^*. When we order the non-zero so that $A_1^* < A_2^*$ always holds, the steady state corresponding to $A = A_2^*$ increases and the steady state corresponding to $A = A_1^*$ decreases with growing λ_0, confirming the statements of Theorems 2.3 and 2.4. These results are reported in Figure 5.

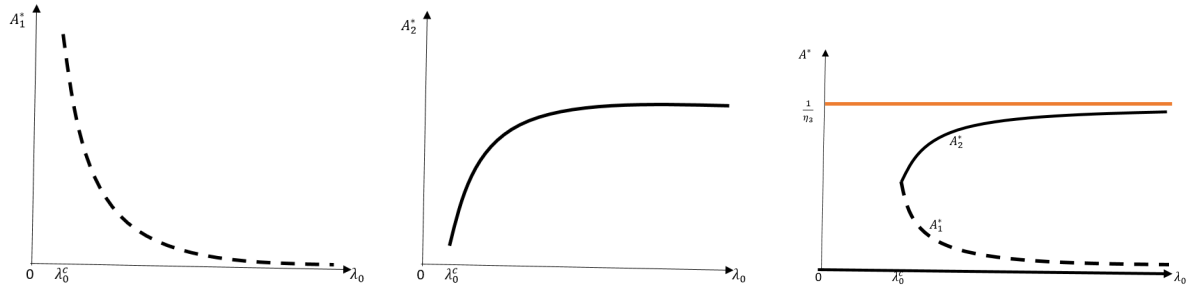

(a) (b) (c)

Figure 5: Diagrams showing the behaviour of the steady-states solutions of system (26) as λ_0 varies. When $\lambda_0 > \lambda_0^c$, the system has two non-trivial equilibria A_1^* and A_2^*. (a) A_1^* is monotone decreasing as a function of λ_0. (b) A_2^* is monotone increasing as a function of λ_0. (c) For $\lambda_0 < \lambda_0^c$, only the trivial equilibrium exists (the solid black line on the horizontal axis). At $\lambda_0 = \lambda_0^c$, a new steady state solution emerges, which then bifurcates into A_1^* (the dashed curve) and A_2^* (the solid curve) for $\lambda_0 > \lambda_0^c$. Equilibrium A_1^* decreases to zero as $\lambda_0 \to \infty$, and A_2^* increases to (in this case) $\frac{1}{\eta_3}$ and the inequality $0 < A_1^* < A_2^* < \frac{1}{\eta_3}$ always holds.

Next, we explore the dependence of the A component of the non-trivial equilibrium on the parameter λ_0. For this, we select an initial condition outside the basin of attraction of the trivial steady state. We hold all other parameters of the system fixed as $a_H = 0.6$, $a_V = 0.3$, $L = 100, L_P = 1000$, $\gamma = 0.7$, $\mu_{A1} = 0.05$, $\theta = 0.5$, $\xi = 0.6$, $\tau_H = 0.2$, $\tau_V = 0.4$, $\mu_{Q_H} = \mu_{Q_V} = \mu_{R_H} = \mu_{R_V} = \mu_B = \mu_{F_B} = 0.04$, $\mu_{M_B} = 0.2$, $p = 0.86$, $q = 0.9$, $S = 0.01$, $\theta_1 = 0.8, V = 10^6$, $H = 10^4$, $\varsigma = 0.5$, $\mu_{A2} = 0.05$ and vary λ_0. For each value of λ_0, we numerically solve (26), then select the value of A at which the values for all state variables stabilise, indicating reaching the equilibrium state. We denote the corresponding value of A by A_∞. The graph of A_∞ against λ_0 is presented in Figure 6 (a). The results again confirm the existence of a threshold value of λ_0, λ_0^c, below which only the trivial steady state exists. As λ_0 increases from zero, and $\mathcal{B} < 1$, only a trivial steady state exists, and it is selected by default because it is also stable. As λ_0 increases further, a saddle-node bifurcation occurs at λ_0^c, after which $\mathcal{B} > 1$, leading to the creation of two non-trivial steady states. The initial condition now deselects the trivial steady state and, at the same time, selects the steady state for which its A component is increasing with respect to λ_0, i.e., the steady state corresponding to $A = A_2^*$ as shown in Figure 6 (a). For illustration, we mark the point $(\lambda_0, A_\infty) = (10, 2.56)$ as shown on Figure 6 (a). With $\lambda_0 = 10$, we numerically integrate the full system to obtain the time series solution curve for A in Figure 6 (b), which is consistent with what we expect from Figure 6 (a). At $\lambda_0 = 10$, $A_1^* = 0.0131388$, $A_2^* = 2.56464$, affirming the stability of the steady state corresponding to A_2^*.

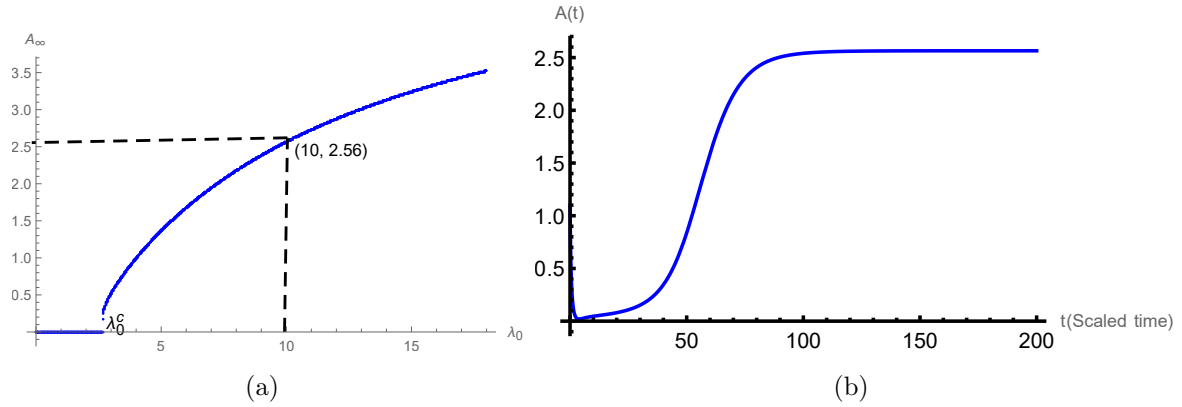

(a) (b)

Figure 6: Numerical exploration of the dependence of the A component of the equilibrium, A_∞, on λ_0. (a) The bifurcation diagram shows that as λ_0 increases from zero, $\mathcal{B} < 1$, A_∞ is 0 and, as λ_0 increases further, a bifurcation occurs at λ_0^c leading to the creation new non-trivial steady states for $\lambda_0 > \lambda_0^c$. At that bifurcation point, the initial condition ceases to be included in the basin of attraction of the trivial equilibrium, and moves to the basin of attraction of the stable non-trivial equilibrium, corresponding to the A branch, which increases with respect to λ_0. (b) Long-term profile of the time series plot of the solution of the A-component of the solution for $\lambda_0 = 10$. It converges to the value of $A_\infty = 2.56$, as marked on the graph in (a).

The stability result illustrated in 6 (b) is local since we can alter the initial conditions so that the dynamics selects the trivial equilibrium, shown in Figs 2 and 3, where we first demonstrated the bi-stability nature of the system. To further understand this concept, we consider initial conditions of the form

$$\boldsymbol{x}_0(A_0) = (A_0, 0, 0, 0, 0, 0, 0, 0)\,, \quad A_0 \in \mathbb{R}_+. \tag{38}$$

With the parameter values used in Figure 6 (b), we consider initial conditions (38) and vary A_0 starting from zero, then plot a graph of A_∞ against A_0, see Figure 8 (a). This graph shows that the sets

$$S_0 = \{\boldsymbol{x}_0(A_0) : A_0 < a_S\} \text{ and } S_* = \{\boldsymbol{x}_0(A_0) : A_0 \geq a_S\} \tag{39}$$

are respectively, subsets of the basin of attraction of the trivial and non-trivial steady states. To confirm this, we numerically solve (26) starting at $\boldsymbol{x}_0(0.2) \in S_0$ and $\boldsymbol{x}_0(1.1) \in S_*$, obtaining the graphs in Figs 7 (a) and (b), respectively.

To investigate how the size of a_S varies as a function of λ_0, we repeat the simulations shown in Figure 8 (a) for different values of λ_0. The points of the set

$$S_S = \{\boldsymbol{x}_0(A_0) : A_0 = a_S\}. \tag{40}$$

are represented by the blue curve on the $A(0) - \lambda_0$ plane in Fig. 8 (b). When $\lambda_0 < \lambda_0^c$, the only stable equilibrium is the trivial equilibrium. For $\lambda_0 \geq \lambda_0^c$, we have two stable steady states, the trivial and non-trivial. In this case, the size of a_S reduces with an increase in λ_0. Hence, the sets S_0 and S_*, respectively, shrink and increase with increase λ_0 and we can partition the $A(0) - \lambda_0$ plane into three regions: S_I, S_{II} and S_{III}, as shown in Fig. 8 (b), so that the following hold: i) $S_I \cup S_{II} \subset S_0$. ii) $S_S \cup S_{III} \subset S_*$

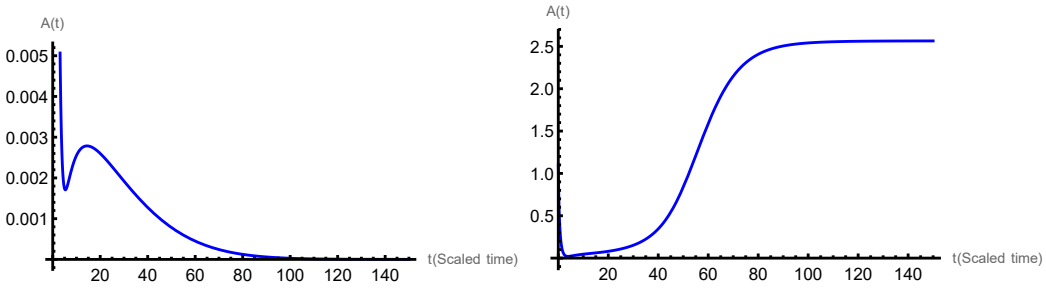

(a) (b)

Figure 7: With the parameter values adopted in this section, we can observe that $\boldsymbol{x}(0.2) = (0.2, 0, 0, 0, 0, 0, 0, 0) \in S_0$, (a), and $\boldsymbol{x}(1.1) = (1.1, 0, 0, 0, 0, 0, 0, 0) \in S_*$, (b).

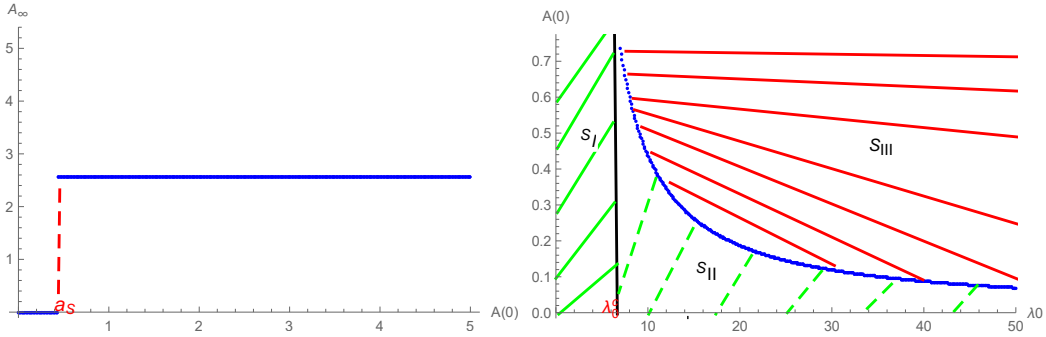

(a) (b)

Figure 8: With the parameter values of this section, we consider initial conditions of the form $\boldsymbol{x}_0(A_0)$ and vary A_0 starting from zero, then plot a graph of A_∞ against A_0, (a). Figure (b) shows that we can partition the $A(0) - \lambda_0$ plane into three regions: S_I, S_{II} and S_{III}. For $\lambda_0 < \lambda_0^c$, we are in the region S_I, for which the trivial steady state is the only stable solution. For $\lambda_0 \geq \lambda_0^c$, we have regions S_{II} and S_{III}. In these two regions, the locally stable trivial steady state coexists with a locally stable non-trivial steady state. For $(\lambda_0, A(0)) \in S_{II}$, the solution will converge to the trivial steady state, while the region S_{III} will give rise to solutions converging to the non-trivial steady state corresponding to A_2^*.

4. Impact of Mating and Alternative Questing Places

In earlier models for mosquito dynamics that incorporated the gonotrophic cycle, such as those in [18, 32, 33], there existed a threshold hold parameter, $\mathcal{R}$, called the basic offspring number, that determined both the existence and stability of equilibrium solutions in the sense that when $\mathcal{R} \leq 1$, the trivial steady state was the only steady state and it was globally asymptotically stable. It became unstable when $\mathcal{R} > 1$, for which values a non-trivial steady state co-existed with the unstable trivial equilibria. The non-trivial equilibrium, which was stable for a range of system parameters, could also be driven to instability via a Hopf bifurcation. The model we propose and study in this paper has yielded results that differ in several ways from those of the earlier models studied in *op. cit.* Namely, (i) the model studied here exhibits a bi-stability (the co-existence of locally stable trivial and non-trivial steady states), absent in previous models of this type, (ii) the threshold parameter $\mathcal{B}$ found here, differs from $\mathcal{R}$ or $\mathcal{N}$ found in the earlier models in that it only affects the existence and size of the steady state solution but does affect their stability, (iii) the model studied here does not display oscillatory dynamics, that is, we have not been able to identify the presence of a Hopf bifurcation, even by using the oviposition functions that are known to lead to it in other models. These novel features likely occur due to the inclusion of alternative blood sources and mating dynamics, factors not considered in the prior models. Next, we investigate whether the observed bi-stability is driven primarily by mating, alternative blood sources, or a combination of both.

4.1. Model with Mating but Without Alternative Blood Sources

We begin investigating the source of bistability by considering (26) with no alternative blood sources. Then, by setting $Q_V = R_V = 0$, (26) reduces to

$$\left.\begin{aligned}
\tfrac{dA}{dt} &= \alpha_1 R_H \lambda \left(\eta_1 L R_H\right)\left(1-\eta_3 A\right) - (\alpha_3 + \alpha_4 A)A, \\
\tfrac{dM_B}{dt} &= \beta_1 \left(A - M_B\right), \\
\tfrac{dF_B}{dt} &= A - M_B F_B - \beta_2 F_B, \\
\tfrac{dB}{dt} &= \theta_1 M_B F_B + \delta_1 R_H - \beta_3 B, \\
\tfrac{dQ_H}{dt} &= \rho_1 \left(B - Q_H\right), \\
\tfrac{dR_H}{dt} &= Q_H - R_H.
\end{aligned}\right\} \tag{41}$$

Theorem 4.1. *Let the birthrate function be either λ_1 or λ_2, defined in* (16) *and* (17)*, respectively. The trivial steady state of system* (41)*, which always exists, is locally asymptotically stable irrespective of the system parameters.*

Proof. See Appendix B.15

Similarly to the results obtained in Section 3, numerical experiments demonstrate that when non-trivial steady states exist, one is stable and coexists with the stable trivial steady state. This shows that alternative blood sources do not introduce the bistability. Instead, alternative blood sources merely increase the chances of mosquito survival, as explained in Section 2.7. The expression for $\mathcal{B}$ reveals that even without humans, alternative blood sources can potentially push the value of $\mathcal{B}$ above its threshold value, leading to mosquito abundance when the starting initial densities of mosquitoes are of the right order of magnitude.

4.2. Model with no Mating and no Alternative Blood Sources

To investigate the effects of including mating into the mosquito dynamics, we revisit equation (2) in terms of the original parameters of the system and assume that aquatic life forms are converted to terrestrial forms at a rate γ, so that a proportion $\xi\gamma$ mature directly into females of type B at the breeding site. If we do not consider alternative blood sources, we have the system

$$\left.\begin{aligned}
\tfrac{dA}{dt} &= \left(a_H R_H + a_V R_V\right) \cdot \lambda(R_H) \cdot \left(1 - \tfrac{A}{L_P}\right) - \left(\gamma + \mu_{A1} + \mu_{A2} A\right) A, \\
\tfrac{dB}{dt} &= \xi\gamma A + a_H R_H - bB - \mu_B B, \\
\tfrac{dQ_H}{dt} &= \kappa^* B - \tau_H H Q_H - \mu_{Q_H} Q_H, \\
\tfrac{dR_H}{dt} &= p\tau_H H Q_H - a_H R_H - \mu_{R_H} R_H.
\end{aligned}\right\} \tag{42}$$

System (42) is the model for mosquito population with no mating ($F_B = M_B = 0$) and no alternative blood sources ($R_V = Q_V = 0$). Similarly to (12), we can rewrite (42) in the form

$$\left.\begin{aligned}
\frac{dA^*}{dt^*} &= \left(\frac{a_H R_H^0 T^0}{A^0}\right) R_H^* \lambda(R_H^0 R_H^*)\left(1 - \frac{A^0 A^*}{L_P}\right) - T^0\left(\gamma + \mu_{A1} + (\mu_{A2} A^0) A^*\right) A^*, \\
\frac{dB^*}{dt^*} &= \left(\frac{\xi\gamma A^0 T^0}{B^0}\right) A^* + \left(\frac{a_H R_H^0 T^0}{B^0}\right) R_H^* - \left((\kappa + \mu_B) T^0\right) B^*, \\
\frac{dQ_H^*}{dt} &= (\tau_H H + \mu_{Q_H}) T^0 \left(\left(\frac{b_H^* B^0}{Q_H^0(\tau_H H + \mu_{Q_H})}\right) B^* - Q_H^*\right), \\
\frac{dR_H^*}{dt^*} &= \left(a_H + \mu_{R_H}\right) T^0 \left(\left(\frac{p\tau_H H Q_H^0}{R_H^0\left(a_H + \mu_{R_H}\right)}\right) Q_H^* - R_H^*\right),
\end{aligned}\right\} \tag{43}$$

then, with an appropriate choice of the parameters: T^0, B^0, Q_H^0 and R_H^0 and dropping the $*'s$, we can scale (43) to take the form analogous to (41),

$$\left.\begin{aligned}
\frac{dA}{dt} &= \alpha_1 R_H \lambda\left(\eta_1 L R_H\right)(1 - A) - (\alpha_3 + \alpha_4 A) A, \\
\frac{dB}{dt} &= A + \delta_1 R_H - \beta_3 B, \\
\frac{dQ_H}{dt} &= \rho_1\left(B - Q_H\right), \\
\frac{dR_H}{dt} &= Q_H - R_H,
\end{aligned}\right\} \tag{44}$$

with $\delta_1 < \beta_3$. To proceed with the analysis of this model, we define the parameter grouping:

$$\hat{\mathcal{B}}_H = \frac{\alpha_1 \lambda(0)}{\alpha_3\left(\beta_3 - \delta_1\right)} = \frac{\alpha_1 \lambda_0}{\alpha_3\left(\beta_3 - \delta_1\right)}. \tag{45}$$

We assume that λ is a continuous, nonnegative decreasing function and $0 < A_0 < 1$ so that $0 < A(t) < 1$. Then we have

Theorem 4.2. *Let the parameter $\hat{\mathcal{B}}_H$ be as defined in* (45)*. Then,*

1. *system* (44) *has a trivial steady state that always exists for all system's parameter values,*
2. *system* (44) *has a unique nontrivial equilibrium if and only if $\hat{\mathcal{B}}_H > 1$,*
3. *the trivial steady state is locally asymptotically stable when $\hat{\mathcal{B}}_H < 1$ and unstable when $\hat{\mathcal{B}}_H > 1$,*
4. *the non-trivial steady state, when it exists, is stable for a range of values of $\hat{\mathcal{B}}_H$, but can also be driven to instability via a Hopf Bifurcation.*

Proof. See Appendix B.16.

This result demonstrates that the bistability observed in (26) will not occur when we suppress both mating and alternative blood sources.

4.3. Model with no Mating but with Alternative Blood Sources

Again, we revisit equation (2) in terms of the original parameters of the system and assume that aquatic lifeforms are converted to terrestrial forms at a rate γ, so that a proportion $\xi\gamma$ matures directly into females of type B at the breeding site. If we keep alternative blood

sources, we have

$$\left.\begin{array}{rcl}
\frac{dA}{dt} &=& (a_H R_H + a_V R_V)\cdot\lambda(R_H,R_V)\cdot\left(1-\frac{A}{L_P}\right) - (\gamma+\mu_{A1}+\mu_{A2}A)\,A,\\
\frac{dB}{dt} &=& \xi\gamma A + a_H R_H + a_V R_V - bB - \mu_B B,\\
\frac{dQ_H}{dt} &=& \kappa_H^* B - \tau_H H Q_H - \mu_{Q_H} Q_H,\\
\frac{dQ_V}{dt} &=& \kappa_V^* B - \tau_V V Q_V - \mu_{Q_V} Q_V,\\
\frac{dR_H}{dt} &=& p\tau_H H Q_H - a_H R_H - \mu_{R_H} R_H,\\
\frac{dR_V}{dt} &=& q\tau_V V Q_v - a_V R_V - \mu_{R_V} R_V,
\end{array}\right\} \tag{46}$$

System (46) is a model for mosquito dynamics with no mating ($F_B \equiv M_B \equiv 0$), but where the mosquito can access multiple questing places. Again, with an appropriate choice of parameter regrouping, we can scale (46) to

$$\left.\begin{array}{rcl}
\frac{dA}{dt} &=& (\alpha_1 R_H + \alpha_2 R_V)\lambda\left(\eta_1 L R_H + \eta_2 L R_V\right)(1-A) - (\alpha_3+\alpha_4 A)A,\\
\frac{dB}{dt} &=& A + \delta_1 R_H + \delta_2 R_v - \beta_3 B,\\
\frac{dQ_H}{dt} &=& \rho_1\left(B - Q_H\right),\\
\frac{dQ_V}{dt} &=& \rho_2\left(B - Q_V\right),\\
\frac{dR_H}{dt} &=& Q_H - R_H,\\
\frac{dR_V}{dt} &=& \rho_3\left(Q_V - R_V\right),
\end{array}\right\} \tag{47}$$

with $\delta_1+\delta_2<\beta_3$. We now re-examine the results of Theorem 4.2 with the following modifications. First, the threshold parameter $\hat{\mathcal{B}}_H$ for this model takes the form

$$\tilde{\mathcal{B}}_{HV} = \frac{(\alpha_1+\alpha_2)\lambda(0)}{\alpha_3\left(\beta_3-\delta_1-\delta_2\right)} = \frac{(\alpha_1+\alpha_2)\lambda_0}{\alpha_3\left(\beta_3-\delta_1-\delta_2\right)}, \tag{48}$$

while the equation $Ah(A)=0$ in (B.32) becomes

$$Ah(A)=0,\quad h(A) = \frac{\alpha_1+\alpha_2}{\beta_3-\delta_1-\delta_2}\lambda\left(\frac{(\eta_1+\eta_2)LA}{\beta_3-\delta_1-\delta_2}\right)(1-A) - (\alpha_3+\alpha_4 A). \tag{49}$$

Then,

1. points 1 and 2 of Theorem 4.2 follows with $\hat{\mathcal{B}}_H$ replaced with $\tilde{\mathcal{B}}_{HV}$,
2. point 3 of Theorem 4.2 can also be verified, since

$$J(\mathbf{0}) = \begin{pmatrix}
-\alpha_3 & 0 & 0 & 0 & \alpha_1\lambda(0) & \alpha_2\lambda(0)\\
1 & -\beta_3 & 0 & 0 & \delta_1 & \delta_2\\
0 & \rho_1 & -\rho_1 & 0 & 0 & 0\\
0 & \rho_2 & 0 & -\rho_2 & 0 & 0\\
0 & 0 & 1 & 0 & -1 & 0\\
0 & 0 & 0 & \rho_3 & 0 & -\rho_3
\end{pmatrix}, \tag{50}$$

and the characteristic polynomial takes the form $p_6(\zeta) = \zeta^6 + a_5\zeta^5 \cdots + a_1\zeta + a_0$, where the sequence of coefficients $\{1, a_5, a_4, a_3, a_2, a_1, a_0\}$ is easily established. In particular, we find $a_0 = \alpha_3\rho_1\rho_2\rho_3\left(\beta_3 - \delta_1 - \delta_2\right)\left(1 - \tilde{\mathcal{B}}_{HV}\right)$, while the others are positive. It is then clear that when $\tilde{\mathcal{B}}_{HV} > 1$, $a_0 < 0$, showing the presence of a positive eigenvalue. Hence, the trivial steady state is unstable whenever $\tilde{\mathcal{B}}_{HV} > 1$.

Therefore, the bistability can not be obtained in this case. We have thus established that mating is the likely cause of the phenomenon of bistability observed in the full model.

Now, the reproductive success of mosquitoes requires behavioural responses by the adult mosquitoes directed towards the location and recognition of mating partners and mating itself. The insect must optimise this aspect of its reproductive life. For anophelines, it is generally accepted that mating occurs within the first 3-5 days of adult female life. While [43] considers a case when most *Anopheles sp.* females take their first blood meal before mating, [9, 10] studies the case when the anopheline rarely takes a blood meal before mating. In some species of mosquitoes, such as *Aedes aegypti*, mating is accompanied by a change of behaviour, caused by the transfer of 'matron', a male hormone, which makes the female refractory to successive matings and instead induces blood questing, see [22, 23, 10, 22, 20]. It is generally believed that in most mosquitoes, the female stores the spermatozoa in spermatheca after copulation so that during each subsequent oviposition, the eggs can be fertilized during their transit through the oviduct and that for the *Anopheles*, males can mate several times but re-mating in females is rare, though has been reported, see [49, 45].

Having an unstable trivial equilibrium state benefits the organisms as driving the population to extinction becomes difficult. Since mating is ubiquitous for the type of fertilisation involved, it is advantageous for the mosquito to mate only once during its entire reproductive life to avoid returning to the bottleneck caused by mating. This is an important result for mosquito dynamics. In the model studied here, mating is successful with probability θ_1, and the insect lives to continue the life cycle, or is killed with probability $1-\theta_1$. This, therefore, makes mating very expensive for the mosquito. Based on the foregoing, the current analysis shows that for an adult female mosquito, it is better to mate once on emergence and then carry on with blood feeding and egg laying as many times as possible. In a general setting, while recognising the fact that mating is a dangerous process, it may be, however, possible to assume that only a fraction of the mosquitoes that did not succeed in mating during the mating encounter die, and the remaining fraction lives to try mating again.

5. Discussion and Conclusion

In this manuscript, we used mathematical modelling to study the role of mating in the dynamics of the mosquito population. We proposed a system of ordinary differential equation that partitioned the mosquito population into aquatic forms (A), newly emerged male and female mosquitoes (M_B and F_B, respectively), fertilized female mosquitoes at breeding sites (B), questing (Q), and fed and resting mosquitoes (R). We assumed that F_B can only transition to type B mosquitoes through mating. The questing mosquitoes were allowed to visit multiple questing places, including both human and non-human sources, where they could quest for blood.

Within this framework, in Section 2, we derived a system of equations describing the population's dynamics. There, we also discussed different ways mating can occur, and finally, we settled on the mass-action mechanism of encounters. We assumed that only a fraction θ_1 of all mating encounters led to successful fertilisation. The parameter θ_1 plays an important role in the mosquito's life as it captures the fact that if many female mosquitoes do not succeed in mating, the population may face extinction. Thus, we can interpret mating as a bottleneck in the sequence of events in the mosquito's life, which can limit the growth of the entire

mosquito population. In the model, we also considered two blood-questing possibilities: human and animal habitats. In the context of mosquito dynamics and disease control, it can give the possibility to study the effects of various techniques preventing human infections, such as the use of Insecticide Treated/Impregnated Nets (ITNs), or zooprophylaxis as a method to decrease human-mosquito interactions. Our model allowed adult mosquitoes to lay eggs directly in an aquatic environment with a possibly finite carrying capacity. Juvenile forms developing in this environment can then mature into male and female mosquitoes that start the terrestrial life stages of the mosquito.

An important aspect of our modelling framework is its ability to quantify the reproductive gains acquired by a mosquito after its interaction with blood sources, which are represented by the oviposition function that measures the density of eggs produced by each reproducing mosquito per unit time. It is customary to assume in the literature that such a function should be a monotone decreasing function of the total size of the reproducing mosquitoes. We observed that the oviposition function should be positive on the admissible domain, as otherwise, we can encounter negative solutions, rendering the model biologically incorrect. In particular, we determined conditions to ensure that a popular logistic function did not generate negative solutions. Such a result has not been established in earlier models of this type.

We rescaled the model for notational convenience and discussed the relative sizes of the scaled parameters. We studied the existence and stability of steady states for the scaled model and presented numerical simulations to provide insight into the solutions of our system when we could not provide analytical results. Analysis of the model revealed the existence of a positive threshold parameter, $\mathcal{B}$, defined in (36), which differs in several ways from threshold parameters that have been identified in mosquito dynamics models, e.g., in [29, 32, 18, 35]. In fact, $\mathcal{B}$ only affects the existence and size of the steady states of the system but does not affect their stability properties. In particular, when $\mathcal{B} \leq 1$, the system has only the trivial steady state and when $\mathcal{B} > 1$, the system now has two nontrivial steady states co-existing with the trivial steady state. In the latter case, the initial conditions determine the long-term behaviour of the solutions depending on the basin of attraction to which they belong. In other words, the system's long-term fate depends on the choice of the initial conditions. We observed that the oviposition parameter λ_0 and the effective fertilisation parameter θ_1 (affecting b) are crucial for the size of $\mathcal{B}$ in the sense that irrespective of the path through which $(\lambda_0, \theta_1) \to (0, 0)$, $\lim_{(\lambda_0,\theta_1)\to(0,0)} \mathcal{B} = 0$, and $\mathcal{B} \to 0$ is a sure pathway to extinction. We note that though other parameters, such as the bio-transition parameters ξ and γ, also affect the size of $\mathcal{B}$ in a similar way, we found λ_0 to be the most convenient bifurcation parameter.

Numerical simulations allowed us to capture some important features of our model by varying $\mathcal{B}$. When $\mathcal{B} \leq 1$, the trivial steady state, which is the only steady state, is globally asymptotically stable. When $\mathcal{B} > 1$, the trivial steady state persists as a locally asymptotically stable equilibrium alongside two non-trivial equilibria (which bifurcate from one equilibrium at $\mathcal{B} = 1$), the larger being stable and the smaller unstable. The system's long-term behaviour is then determined by the basin of attraction the initial condition belongs to. We note that analytical confirmation of these results for a class of considered models has been achieved by a combination of asymptotic analysis and methods of monotone systems in [7].

We note that the bistability, a mathematical term for the Allee effect, is quite common in insect populations, [15], and has been studied in some simpler mosquito population models, see, e.g., [27, 25, 48, 41]. In all these papers, however, the Allee effect was introduced by a suitable modification of the mating or oviposition mechanism. Here, we begin with a more complex system but with a simple mass-action mating mechanism, [40], and examine the impact of different features of the model, such as alternative blood sources or mating, on its long-term dynamics, establishing that the bistability is a natural consequence of sexual reproduction. We concluded that to increase the species' survival chances, it is advantageous for a mosquito to

mate only once and then lay as many eggs as possible. Our findings highlight the following key insights:

1. **Allee Effect**: In contrast to models without mating [32, 18], the trivial steady state in our model incorporating mating is always locally asymptotically stable. Moreover, if a non-trivial steady state exists, the long-term dynamics of the system depends on its initial size. This property resembles the Allee effect in one-dimensional systems: if the initial mosquito population is very small, the system is unsustainable. Conversely, sufficiently large populations survive.
2. **Targeting Mating**: The model suggests that interfering with the mating process is a highly effective strategy for suppressing mosquito populations at low densities. This is evident from the nature of $\mathcal{B}$. Reducing the effectiveness of mating by making $\theta_1 \ll 1$ makes $\mathcal{B} < 1$, which yields the extinction of mosquito populations.

Due to the complexity of the model, we could only present numerical studies of the stability results of the non-trivial steady state and the existence of the basins of attractions for the trivial and non-trivial equilibria. However, a class of models of this type can be studied using multiscale analysis and monotonicity methods; see [7], and the analytical results obtained there confirm the observations formulated in this paper and based on numerical simulations. It is our understanding that, given the nature of the environment in which mosquitoes live and breed, a more appropriate framework to study their population dynamics should include elements of stochasticity, climatic factors, as well as spatial considerations. It will also be beneficial to fit and validate our model with data, and as such relate the aspects of bistability studied here to the real world. These and many other aspects of the mosquito control problem, are aspects under consideration to be presented elsewhere.

Acknowledgements: BMG, GAN and JB acknowledge financial support from the National Research Foundation (NRF), South Africa and the DST/NRF SARChI Chair in Mathematical Models and Methods in Biosciences and Bioengineering, University of Pretoria, South Africa, that enabled all three to meet in Pretoria in 2024 when most of the work was done. GAN and BMG also acknowledge support for the Cameroonian Ministry of Higher Education through the initiative for the modernisation of research in Cameroon's Higher Education for 2023 and 2024. BMG, MIT and GAN acknowledge the sponsorship of the Commission for Developing Countries (CDC) in conjunction with the International Mathematics Union (IMU) through the CDC-ADMP (African Diaspora Mathematicians Program) grant that made it possible for interactive collaborative work during the 2018 and 2019 grant sponsored visits to the University of Buea by MIT-E during which period some aspects of this work was discussed.

Appendix A. Scaling

Here, we present details of the scaling process. Let $t = T^0 t^*$, $R_H = R_H^0 R_H^*$, $R_V = R_H^0 R_V^*$, $A = A^0 A^*$, $M_B = M_B^0 M_B^*, F_B = F_B^0 F_B^*$, $B = B^0 B^*$, $Q_H = Q_H^0 Q_H^*$, $Q_V = Q_V^0 Q_V^*$

so that (12) becomes

$$\left.\begin{aligned}
\tfrac{dA^*}{dt^*} &= \left(\left(\tfrac{a_H R_H^0 T^0}{A^0}\right) R_H^* + \left(\tfrac{a_V R_V^0 T^0}{A^0}\right) R_V^*\right) \lambda (R_V^0 R_V^* + R_H^0 R_H^*) \left(1 - \tfrac{A^0 A^*}{L_P}\right) \\
&- T^0 \left(\gamma + \mu_{A1} + (\mu_{A2} A^0) A^*\right) A^*, \\
\tfrac{dM_B^*}{dt^*} &= \left(\tfrac{(1-\theta)\xi\gamma T^0 A^0}{M_B^0}\right) A^* - (\mu_{M_B} T^0) M_B^*, \\
\tfrac{dF_B^*}{dt^*} &= \left(\tfrac{\theta\xi\gamma T^0 A^0}{F_B^0}\right) A^* - (S M_B^0 T^0) M_B^* F_B^* - (\mu_{F_B} T^0) F_B^*, \\
\tfrac{dB^*}{dt^*} &= \theta_1 \left(\tfrac{S M_B^0 F_B^0 T^0}{B^0}\right) M_B^* F_B^* + \left(\tfrac{a_H R_H^0 T^0}{B^0}\right) R_H^* + \left(\tfrac{a_V R_V^0 T^0}{B^0}\right) R_V^* - ((\kappa + \mu_B) T^0)\, B^*, \\
\tfrac{dQ_H^*}{dt} &= \left(\tfrac{\kappa_H^* B^0 T^0}{Q_H^0}\right) B^* - \left(\tfrac{\tau_H H Q_H^0 T^0}{Q_H^0}\right) Q_H^* - (\mu_{Q_H} T^0) Q_H^*, \\
\tfrac{dQ_V^*}{dt} &= \left(\tfrac{\kappa_V^* B^0 T^0}{Q_V^0}\right) B^* - \left(\tfrac{\tau_V V Q_V^0 T^0}{Q_V^0}\right) Q_V^* - (\mu_{Q_V} T^0) Q_V^*, \\
\tfrac{dR_H^*}{dt^*} &= \left(\tfrac{p\tau_H H Q_H^0 T^0}{R_H^0}\right) Q_H^* - \left((a_H + \mu_{R_H})\, T^0\right) R_H^*, \\
\tfrac{dR_V^*}{dt^*} &= \left(\tfrac{q\tau_V V Q_V^0 T^0}{R_V^0}\right) Q_V^* - \left((a_V + \mu_{R_V})\, T^0\right) R_V^*,
\end{aligned}\right\} \quad \text{(A.1)}$$

where $\kappa_H^* = \kappa\left(\frac{H}{H+\varsigma V}\right)$, $\kappa_V^* = \kappa\left(\frac{\varsigma V}{H+\varsigma V}\right)$. Terms in (A.1) can be grouped to have (A.2) below.

$$\left.\begin{aligned}
\tfrac{dA^*}{dt^*} &= \left(\left(\tfrac{a_H R_H^0 T^0}{A^0}\right) R_H^* + \left(\tfrac{a_V R_V^0 T^0}{A^0}\right) R_V^*\right) \lambda (R_V^0 R_V^* + R_H^0 R_H^*) \left(1 - \tfrac{A^0 A^*}{L_P}\right) \\
&- T^0 \left(\gamma + \mu_{A1} + (\mu_{A2} A^0) A^*\right) A^*, \\
\tfrac{dM_B^*}{dt^*} &= (\mu_{M_B} T^0) \left(\left(\tfrac{(1-\theta)\xi\gamma A^0}{M_B^0 \mu_{M_B}}\right) A^* - M_B^*\right), \\
\tfrac{dF_B^*}{dt^*} &= \left(\tfrac{\theta\xi\gamma T^0 A^0}{F_B^0}\right) A^* - (S M_B^0 T^0) M_B^* F_B^* - (\mu_{F_B} T^0) F_B^*, \\
\tfrac{dB^*}{dt^*} &= \theta_1 \left(\tfrac{S M_B^0 F_B^0 T^0}{B^0}\right) M_B^* F_B^* + \left(\tfrac{a_H R_H^0 T^0}{B^0}\right) R_H^* + \left(\tfrac{a_V R_V^0 T^0}{B^0}\right) R_V^* - ((\kappa + \mu_B) T^0)\, B^*, \\
\tfrac{dQ_H^*}{dt} &= (\tau_H H + \mu_{Q_H}) T^0 \left(\left(\tfrac{\kappa_H^* B^0}{Q_H^0 (\tau_H H + \mu_{Q_H})}\right) B^* - Q_H^*\right), \\
\tfrac{dQ_V^*}{dt} &= (\tau_V V + \mu_{Q_V}) T^0 \left(\left(\tfrac{\kappa_V^* B^0}{Q_V^0 (\tau_V V + \mu_{Q_V})}\right) B^* - Q_V^*\right), \\
\tfrac{dR_H^*}{dt^*} &= (a_H R_H^0 + \mu_{R_H})\, T^0 \left(\left(\tfrac{p\tau_H H Q_H^0}{R_H^0 \left(a_H + \mu_{R_H}\right)}\right) Q_H^* - R_H^*\right), \\
\tfrac{dR_V^*}{dt^*} &= (a_V + \mu_{R_V})\, T^0 \left(\left(\tfrac{q\tau_V V Q_V^0}{R_V^0 \left(a_V + \mu_{R_V}\right)}\right) Q_V^* - R_V^*\right).
\end{aligned}\right\} \quad \text{(A.2)}$$

Set

$$\begin{aligned}
T^0 &= \frac{1}{a_H+\mu_{R_H}}, M_B^0 = \frac{1}{ST^0} = \frac{a_H+\mu_{R_H}}{S},\\
A^0 &= \frac{M_B^0\mu_{M_B}}{(1-\theta)\xi\gamma} = \frac{M_B^0\mu_{M_B}}{(1-\theta)\xi\gamma} = \frac{(a_H+\mu_{R_H})\mu_{M_B}}{S(1-\theta)\xi\gamma}, \quad F_B^0 = \theta\xi\gamma A^0T^0 = \left(\frac{\theta}{1-\theta}\right)\left(\frac{\mu_{M_B}}{S}\right)\\
B^0 &= SM_B^0F_B^0T^0 = \left(\frac{\theta}{1-\theta}\right)\left(\frac{\mu_{M_B}}{S}\right) = F_B^0,\\
Q_H^0 &= \frac{\kappa_H^*B^0}{\tau_HH+\mu_{Q_H}} = \left(\frac{\kappa_H^*}{\tau_HH+\mu_{Q_H}}\right)\left(\frac{\theta}{1-\theta}\right)\left(\frac{\mu_{M_B}}{S}\right),\\
Q_V^0 &= \frac{\kappa_V^*B^0}{\tau_VV+\mu_{Q_V}} = \left(\frac{\kappa_V^*}{\tau_VV+\mu_{Q_V}}\right)\left(\frac{\theta}{1-\theta}\right)\left(\frac{\mu_{M_B}}{S}\right),\\
R_H^0 &= \frac{p\tau_HHQ_H^0}{a_H+\mu_{R_H}} = p\left(\frac{\tau_HH}{\tau_HH+\mu_{Q_H}}\right)\left(\frac{\kappa_H^*}{a_H+\mu_{R_H}}\right)\left(\frac{\theta}{1-\theta}\right)\left(\frac{\mu_{M_B}}{S}\right)\\
R_V^0 &= \frac{q\tau_VVQ_V^0}{a_V+\mu_{R_V}} = q\left(\frac{\tau_VV}{\tau_VV+\mu_{Q_V}}\right)\left(\frac{\kappa_V^*}{a_V+\mu_{R_V}}\right)\left(\frac{\theta}{1-\theta}\right)\left(\frac{\mu_{M_B}}{S}\right)
\end{aligned}$$

to get the parameters in (25).

Appendix B. Proofs of key results

Appendix B.1. Proof of Proposition 2.1

If $L_P < \infty$ and $0 < A_0 < L_P$, then $\frac{dA}{dt} < 0$ at $A = L_P$ and hence $A(t)$ is bounded by L_P, therefore $\left(1 - \frac{A(t)}{L_P}\right) > 0$ for all $t \geq 0$. Then, by assumption, for all $0 < L_P \leq \infty$, the oviposition term is always nonnegative and the nonnegativity of solutions of (12) follows directly from [39, Theorem B.7] or [6, Theorem B.21].

By assumption, there is $L_1 < \infty$ be such that $A(t) \leq L_1$ for all $t \geq 0$. Using the nonnegativity of N and $L = \max\{L_1, L_P\}$, we have

$$\frac{dN}{dt} \leq \gamma\xi L - \mu_{min}N, \tag{B.1}$$

$\mu_{min} = \min\{\mu_{F_B}, \mu_{M_B}, \mu_B, \mu_{Q_H}, \mu_{Q_V}, \mu_{R_V}, \mu_{R_H}\}$, and hence

$$N(t) \leq N(0)e^{-\mu_{min}t} + \frac{\gamma\xi L}{\mu_{min}} - \frac{\gamma\xi L}{\mu_{min}}e^{-\mu_{min}t}, \tag{B.2}$$

which means that all components of the solution are bounded. Hence, using, e.g., [6, Theorem B.14], the solutions are are defined for $t \in [0, \infty)$. □

Appendix B.2. Proof of Lemma 2.1

We observe that if $x_{i0} > 0$ for some i, then, by continuity, $x_i(t) > 0$ on some interval $[0, \delta)$. In particular, if $\boldsymbol{J}_0 \gg \mathbf{0}$, then $\boldsymbol{J}(t) \gg \mathbf{0}$ on some $[0, \delta)$.

Lets first consider $i = 4$, that is, $B(t) > 0$ on some interval $[0, \delta)$. Using the variation of constants formula for the non-homogeneous linear Cauchy problem $y' = -ay + f, y(0) = y_0$:

$$y(t) = y_0e^{-at} + e^{-at}\int_0^t e^{as}f(s)ds, \tag{B.3}$$

we get $x_j(t) > 0$ on $(0, \delta)$ for $5 \leq j \leq 8$. Let $\boldsymbol{Y}_{Q0} > 0$, then $p\tau_HHQ_{H0} + q\tau_VVQ_{H0} > 0$. If either $R_{H0} > 0$ or $R_{V0} > 0$, then, by continuity, there is an interval $[0, \delta)$ on which both $R(t) > 0$ and

$a_H R_H(t) + a_V R_V(t) > 0$ and $R(t) < L$. If $R_{H0} = R_{V0} = 0$, adding the last two equations in (12), we obtain

$$\left.\frac{dR}{dt}\right|_{t=0} = p\tau_H H Q_{H0} + q\tau_V V Q_{H0} > 0,$$

and again, $R(t) > 0$, $a_H R_H(t) + a_V R_V(t) > 0$ and $R(t) < L$ on some interval.

Summarizing, if $x_{i0} > 0$ for some $i \geq 4$, then $R(t) > 0$, $a_H R_H(t) + a_V R_V(t) > 0$ and $R(t) < L$ on some interval $(0, \delta)$. Next, we re-write the first equation of (12) as

$$\frac{dA}{dt} = G(t) - \left(\frac{G(t)}{L_P} + \gamma + \mu_{A1} + \mu_{A2} A\right) A,$$

where $G(t) := (a_H R_H(t) + a_V R_V(t))\lambda(R(t)) > 0$ on $(0, \delta)$. Then, if $A_0 = 0$,

$$A(t) = e^{-\int_0^t \left(\frac{G(s)}{L_P} + \gamma + \mu_{A1} + \mu_{A2} A(s)\right) ds} \int_0^t e^{\int_0^s \left(\frac{G(\sigma)}{L_P} + \gamma + \mu_{A1} + \mu_{A2} A(\sigma)\right) d\sigma} G(s) ds > 0 \tag{B.4}$$

on $(0, \delta)$.

If $A_0 > 0$, then, irrespective of $G(t)$, $A(t) > 0$ on some, possibly smaller interval. In either case, using the variation of constants formula again, we have $M_B(t) > 0$ on $(0, \delta)$. Then, as above, we write the solution to the third equation of (12) as

$$\begin{aligned} F_B(t) &= F_B(0) e^{-\mu_{F_B} t - S\int_0^t M_B(s) ds} + \theta\xi\gamma e^{-\mu_{F_B} t - S\int_0^t M_B(s) ds} \int_0^t e^{\mu_{F_B} s + S\int_0^s M_B(\sigma) d\sigma} A(s) ds \\ &\geq e^{-S\int_0^\delta M_B(s) ds} \left(F_B(0) e^{-\mu_{F_B} t} + \theta\xi\gamma e^{-\mu_{F_B} t} \int_0^t e^{\mu_{F_B} s} A(s) ds \right) > 0, \quad t \in (0, \delta], \end{aligned}$$

where, by $M_B(\sigma) > 0$ on $(0, \delta)$, we have

$$e^{S\int_0^s M_B(\sigma) d\sigma} \geq 1, \quad s \leq t \leq \delta.$$

Hence, as before, $F_B(t) > 0$ on $(0, \delta)$. In particular, $M_B(t) > 0$ and $F_B(t) > 0$ irrespective of other initial conditions if (21b) is satisfied.

Now, we write the last five equations of (12) as a non-homogeneous linear system,

$$\boldsymbol{Y}'(t) = \boldsymbol{\mathcal{A}} \boldsymbol{Y}(t) + \boldsymbol{F}(t), \quad \boldsymbol{Y}(0) = \boldsymbol{Y}_0, \tag{B.5}$$

where

$$\boldsymbol{\mathcal{A}} = \begin{pmatrix} -\kappa - \mu_B & 0 & 0 & a_H & a_V \\ \kappa\left(\frac{H}{H+\varsigma V}\right) & -\tau_H H - \mu_{Q_H} & 0 & 0 & 0 \\ \kappa\left(\frac{\varsigma V}{H+\varsigma V}\right) & 0 & -\tau_V V - \mu_{Q_V} & 0 & 0 \\ 0 & p\tau_H H & 0 & -a_H - \mu_{R_H} & 0 \\ 0 & 0 & q\tau_V V & 0 & -a_V - \mu_{R_V} \end{pmatrix},$$

$$\boldsymbol{F} = \begin{pmatrix} \theta_1 S M_B F_B \\ 0 \\ 0 \\ 0 \\ 0 \end{pmatrix},$$

whose solution is given by

$$\boldsymbol{Y}(t) = e^{t\mathcal{A}}\boldsymbol{Y}_0 + \int_0^t e^{(t-s)\mathcal{A}}\boldsymbol{F}(s)ds. \tag{B.6}$$

Since $\mathcal{A}$ is a Metzler matrix, $e^{t\mathcal{A}} \geq 0$ and, if some $x_{i0} > 0, i \geq 4$, (ensuring $G(t) \geq 0$ in (B.4)), or $A_0 > 0$, or $\boldsymbol{J}_0 \gg \boldsymbol{0}$, (ensuring $\boldsymbol{F}(t) \geq \boldsymbol{0}$), then $\boldsymbol{Y}(t) \geq \boldsymbol{0}$ on $(0, \delta)$. In particular, also in the two last cases, $a_H R_H(t) + a_V R_V(t) \geq 0$ on this interval. Hence,

$$\frac{dB}{dt} \geq \theta_1 S M_B F_B - \kappa B - \mu_B B,$$

and the variation of constants formula ensures $B(t) > 0$ on $(0, \delta)$, which gives the positivity of Q_H and Q_V, and of R_H and R_V, on some $(0, \delta)$, and the cycle is complete. □

Appendix B.3. Proof Lemma 2.2

By [39, Theorem B.7], $\boldsymbol{x}(t) \geq \boldsymbol{0}$ as long as $R(t) \in [0, L]$, and, by the previous lemma, $a_H R_H(t) + a_V R_V(t) > 0$ on some $(0, \delta)$. Assume that $R(t_0) = 0$ for some t_0 and $R(t) \leq L$ for $t \in [0, t_0]$. From (B.4), we see that $A(t_0) > 0$. Hence, we can argue similarly to the previous lemma to obtain $R_H(t) > 0$ and $R_V(t) > 0$ on $(t_0, t_0 + \delta)$. □

Appendix B.4. Proof of Lemma 2.3

Using the non-negativity of solutions and (B.3), we obtain

$$\begin{aligned} 0 \leq M_B(t) &\leq \max\left\{M_{B0}, \frac{(1-\theta)\xi\gamma}{\mu_{M_B}} A_M\right\}, \\ 0 \leq F_B(t) &\leq \max\left\{F_{B0}, \frac{\theta\xi\gamma}{\mu_{F_B}} A_M\right\}. \end{aligned} \tag{B.7}$$

Then, we can estimate (B.6) as

$$\|\boldsymbol{Y}(t)\| \leq |||e^{t\mathcal{A}}|||\|\boldsymbol{Y}_0\| + |||e^{t\mathcal{A}}||| \int_0^t |||e^{-s\mathcal{A}}|||\|\boldsymbol{F}(s)\|ds, \tag{B.8}$$

where $|||\cdot|||$ is the operator norm induced by the norm $\|\cdot\|$ in $\mathbb{R}^5$, see, for example, [6, Appendix A1]. A convenient norm here is the l^1-norm on $\mathbb{R}^5$, see (18). For non-negative solutions, we have

$$\|\boldsymbol{Y}(t)\|_1 = B(t) + Q_H(t) + Q_V(t) + R_H(t) + R_V(t),$$

and hence, by adding the equations,

$$\|\boldsymbol{Y}(t)\|_1' \leq -\mu\|\boldsymbol{Y}(t)\|_1, \tag{B.9}$$

where

$$\mu = \min\{-\mu_B, ((1-p)\tau_H H + \mu_{Q_H}, ((1-q)\tau_V V + \mu_{Q_V}, \mu_{R_H}, \mu_{R_V}\} > 0.$$

This means that $|||e^{t\mathcal{A}}||| \le e^{-\mu t}$. Hence, using (B.8) and (B.7),

$$
\begin{aligned}
R(t) &\le \|\boldsymbol{Y}(t)\|_1 \le e^{-\mu t}\|Y_0\|_1 + e^{-\mu t}\int_0^t e^{\mu s}\|\boldsymbol{F}(s)\|_1 ds \\
&\le \max\left\{\|\boldsymbol{Y}_0\|_1, \frac{\theta_1 S}{\mu}\max\left\{M_{B0}, \frac{(1-\theta)\xi\gamma}{\mu_{M_B}}A_M\right\}\max\left\{F_{B0}, \frac{\theta\xi\gamma}{\mu_{F_B}}A_M\right\}\right\} \\
&= \max\left\{\|\boldsymbol{Y}_0\|_1, \frac{\theta_1 S}{\mu}M_{B0}F_{B0}, \frac{\theta_1 S}{\mu}\frac{\theta\xi\gamma}{\mu_{F_B}}M_{B0}A_M, \frac{\theta_1 S}{\mu}\frac{(1-\theta)\xi\gamma}{\mu_{M_B}}F_{B0}A_M, \frac{\theta_1 S}{\mu}\frac{\theta(1-\theta)\xi^2\gamma^2}{\mu_{F_B}\mu_{M_B}}A_M^2\right\}.
\end{aligned}
$$

□

Appendix B.5. Proof of Lemma 2.4

Consider

$$\psi(R_H, R_V) := \lambda_0(a_H R_H + a_V R_V)\left(1 - \frac{R_H + R_V}{L}\right), \quad 0 \le R_H + R_V \le L.$$

It is a continuous function on a compact set, so it achieves a maximum. We see that it is attained at the boundary if $a_H \neq a_V$ or along the line $R_H + R_V = L$ otherwise; in both cases it is given by

$$\Psi := \frac{\max\{a_V, a_H\}\lambda_0 L}{4}.$$

Thus, we obtain

$$A' \le \Psi - (\gamma + \mu_1 + \mu_2 A)A.$$

Considering the quadratic function on the right-hand side, we find its roots to be

$$\lambda_\pm(L) = \frac{\frac{\gamma+\mu_1}{\mu_2} \pm \sqrt{\left(\frac{\gamma+\mu_1}{\mu_2}\right)^2 + \frac{\max\{a_V,a_H\}\lambda_0 L}{\mu_2}}}{2}.$$

The parabola is directed downwards, so the solution for any $0 < A_0 < \lambda_+(L)$, converges to $\lambda_+(L)$ in an increasing way and decreases to it if $A_0 > \lambda_+(L)$. □

Appendix B.6. Proof of Corollary 2.2

We should ensure that

$$L > R_{\max}\left(\max\left\{A_0, \frac{\frac{\gamma+\mu_1}{\mu_2} + \sqrt{\left(\frac{\gamma+\mu_1}{\mu_2}\right)^2 + \frac{\max\{a_V,a_H\}\lambda_0 L}{\mu_2}}}{2}\right\}\right). \tag{B.10}$$

The problem is that L appears on both sides of the above inequality. Hence, we consider

$$\lim_{L\to\infty}\frac{R_{\max}\left(\max\left\{A_0, \frac{\frac{\gamma+\mu_1}{\mu_2} + \sqrt{\left(\frac{\gamma+\mu_1}{\mu_2}\right)^2 + \frac{\max\{a_V,a_H\}\lambda_0 L}{\mu_2}}}{2}\right\}\right)}{L} = \frac{\theta_1 S\theta(1-\theta)\xi^2\gamma^2\lambda_0\max\{a_H, a_V\}}{\mu_{F_B}\mu_{M_B}\mu\mu_2}.$$

Hence, if (24) is satisfied, then there is L^* such that for any $L > L^*$ the estimate (B.10) holds. □

Appendix B.7. Proof of Theorem 2.1

First, we note that the parameters c and b are positive by Remark 2.2, point (6). Set the right-hand side of (26) to zero and solve. From the last four equations, we get

$$B^* = Q_H^* = Q_V^* = R_H^* = R_V^*. \tag{B.11}$$

Substituting (B.11) in the first four equations of (26) gives $A^* = M_B^*$, $F_B^* = \frac{A^*}{A^*+\beta_2} = \frac{M_B^*}{M_B^*+\beta_2}$ and

$$\left.\begin{array}{ll} (i) & R_H^*(\alpha_1+\alpha_2)(1-\eta_3 A^*)\cdot\lambda\left(LR_H^*(\eta_1+\eta_2)\right) - \left(\alpha_3+\alpha_4 A^*\right)A^* = 0, \\ (ii) & \theta_1 A^*\left(\frac{A^*}{A^*+\beta_2}\right) + \delta_1 R_H^* + \delta_2 R_H^* - \beta_3 R_H^* = 0. \end{array}\right\} \tag{B.12}$$

Solving the above gives (30). It is evident that $E_0^* = \mathbf{0}$ solves (29) and (30). □

Appendix B.8. Proof of Lemma 2.5

We simplify

$$g(A) = \frac{(\alpha_3+\alpha_4 A)(A+\beta_2)}{bA(1-\eta_3 A)} = \frac{\alpha_4 A^2 + (\alpha_3+\alpha_4\beta_2)A + \alpha_3\beta_2}{bA(1-\eta_3 A)} \tag{B.13}$$

by defining $z = \eta_3 A$ and

$$\hat{g}(z) := H\frac{z^2+Ez+F}{z(1-z)} =: HG(z),$$

where $H = \alpha_4/b\eta_3, E = (\alpha_3+\alpha_4\beta_2)\eta_3/\alpha_4, F = \eta_3^2\alpha_3\beta_2/\alpha_4$, and, noting that the constant H does not alter the analysed properties, we continue with G. We have

$$G'(z) = \frac{(1+E)z^2+2Fz-F}{z^2(1-z)^2} = \frac{\Phi(z)}{z^2(1-z)^2},$$

and, noting $\Phi(0) = -F < 0$, $\Phi(1) = 1+E+2F > 0, \Phi'(z) > 0$ on $[0,1]$, we see that there is a unique $z_m \in (0,1)$ such that $G'(z_m) = 0$. Thus, $G(z)$ is strictly decreasing from $+\infty$ to $G(z_m)$ on $(0, z_m)$ and strictly increasing from $G(z_m)$ to $+\infty$ on $(z_m, 1)$. Now,

$$G''(z) = 2\frac{(1+E)z^3+3Fz^2-3Fz+F}{z^3(1-z)^3}$$

and we observe that the term $\phi(z) = 3Fz^2 - 3Fz$ is negative on $(0,1)$. However, the minimum of ϕ, attained at $z = \frac{1}{2}$, is $-\frac{3F}{4}$. Hence, $\phi(z) + F \geq \frac{F}{4} > 0$ and $G'' > 0$ on $(0,1)$, so g is strictly concave upwards. □

Appendix B.9. Proof of Theorem 2.2

In the notation of Lemma 2.5, we find

$$A_m^* = \left(\frac{\alpha_3\beta_2}{\sqrt{\alpha_3\beta_2\left(\alpha_3+\frac{\alpha_4}{\eta_3}\right)\left(\beta_2+\frac{1}{\eta_3}\right)} + \alpha_3\beta_2}\right)\frac{1}{\eta_3}. \tag{B.14}$$

At the point $A^* = A_m^*$, $g(A^*)$ attains a minimum

$$g_m := g(A_m^*) = \frac{2\sqrt{\alpha_3\beta_2\left(\alpha_3\eta_3+\alpha_4\right)\left(\beta_2\eta_3+1\right)} + \beta_2\left(2\alpha_3\eta_3+\alpha_4\right) + \alpha_3}{b}. \tag{B.15}$$

Now, since λ is continuous and strictly decreasing, a necessary condition for $\lambda\left(LR_H^*(\eta_1+\eta_2)\right) = g(A^*)$ to have a solution is that $g_m < \lambda(0) = \lambda_0$. We rearrange this solvability condition with g_m from (B.15) using (31) as

$$\frac{2\sqrt{\alpha_3\beta_2\left(\alpha_3\eta_3+\alpha_4\right)\left(\beta_2\eta_3+1\right)}+\beta_2\left(2\alpha_3\eta_3+\alpha_4\right)+\alpha_3}{b} < \lambda_0 \Rightarrow \frac{(\alpha_1+\alpha_2)\theta_1\lambda_0}{(\alpha_3+\nu)(\beta_3-\delta_1-\delta_2)} > 1, \tag{B.16}$$

where

$$\nu = 2\sqrt{\alpha_3\beta_2\left(\alpha_3\eta_3+\alpha_4\right)\left(\beta_2\eta_3+1\right)}+\beta_2\left(2\alpha_3\eta_3+\alpha_4\right).$$

This gives a threshold parameter

$$\mathcal{B}_\lambda = \frac{(\alpha_1+\alpha_2)\theta_1\lambda_0}{(\alpha_3+\nu)(\beta_3-\delta_1-\delta_2)} = \frac{b\lambda_0}{\alpha_3+\nu}, \tag{B.17}$$

see (31), so that we can conclude that $\mathcal{B}_\lambda > 1$ is a necessary condition for the steady state equation to have at least one positive solution within the required interval. Further, if $0 \leq \mathcal{B}_\lambda \leq 1$, then $\lambda(0)$ is below or at the same level as g_m, which, having in mind that λ is strictly decreasing, precludes the existence of non-trivial solutions. □

Appendix B.10. Proof of Theorem 2.3

The non-trivial steady states are obtained by solving the equation

$$\sigma\frac{A^{*2}}{A^*+\beta_2} = \lambda^{-1}\left(g(A^*)\right), \tag{B.18}$$

where $\sigma = c(\eta_1+\eta_2)$ and g was defined in (B.13). In this case, $\lambda^{-1}(R) = \frac{L(\lambda_0-R)}{R}$, so that (B.18) takes the form

$$\sigma A^{*2}\left(A^*\alpha_4+\alpha_3\right) = b\lambda_0 A^*\left(1-\eta_3 A^*\right) - \left(\alpha_3+\alpha_4 A^*\right)\left(A^*+\beta_2\right), \tag{B.19}$$

which can be transformed to

$$\begin{aligned} &P_3(A) = a_3A^3+a_2A^2+a_1A+a_0, \quad \text{where} \\ &a_0 = \alpha_3\beta_2 > 0, \quad a_1 = \alpha_4\beta_2+\alpha_3-b\lambda_0, \quad a_2 = \alpha_4+b\eta_3\lambda_0+\alpha_3\sigma > 0, \\ &a_3 = \alpha_4\sigma > 0. \end{aligned} \tag{B.20}$$

The discriminant of P_3 can be calculated as, [38],

$$\Delta = -4a_3a_1^3+a_2^2a_1^2+18a_3a_2a_0a_1-27a_3^2a_0^2-4a_2^3a_0.$$

$\Delta > 0$ is a necessary and sufficient condition for three distinct real roots to exist (if $\Delta = 0$, then we have a double root, automatically real). Consider now $z = -a_1 = b\lambda_0-\alpha_4\beta_2-\alpha_3$ and

$$\Psi(z) = 4a_3z^3+a_2^2z^2-18a_3a_2a_0z-27a_3^2a_0^2-4a_2^3a_0, \quad z \geq 0.$$

Then $\Psi(0) < 0$, $\lim_{z\to\infty}\Psi(z) = \infty$, and

$$\Psi'(z) = 12a_3z^2+2a_2^2z-18a_3a_2a_0.$$

Then, $\Psi'(z)$ has only one positive root and $\Psi'(0) < 0$. Consequently, $\Psi(z)$ has only one stationary point for $z_{\min} > 0$ and, since $\Psi(z)$ is decreasing at $z = 0$, it must be a minimum. Then, for $z > z_{\min}$, $\Psi(z)$ is increasing to ∞. Hence, there is a unique $z^* > 0$ for which $\Psi(z^*) = 0$. In

other words, there is a unique $b^*\lambda_0^*$ such that if

$$\alpha_4\beta_2 + \alpha_3 \leq b\lambda_0 < b^*\lambda_0^*, \tag{B.21}$$

then $\Delta < 0$, and so there must be two complex roots P_3, and if

$$b^*\lambda_0^* \leq b\lambda_0, \tag{B.22}$$

then $\Delta \geq 0$ and hence all roots of P_3 are real.

First, we observe that $P_3(0) = a_0 > 0$; thus, P_3 has a negative root. First, we consider what happens if $b\lambda_0 < \alpha_4\beta_2 + \alpha_3$, that is, $a_1 > 0$. Then there are no positive solutions as $P_3' > 0$ for $A > 0$. So, assume $b\lambda_0 \geq \alpha_4\beta_2 + \alpha_3$, as above. Then, we can focus on the case (B.22), as otherwise, the only real solution is negative. Since, in this case, $a_1 < 0$, we have two sign changes, and Descartes's rule of signs ensures that $P_3(A)$ has either two or no positive real roots. Since all roots are real, we have either three negative roots or two positive roots. In the former case, $P_3(A)$ must increase for A larger than the largest negative root, so, in particular, $P_3'(0) > 0$. On the other hand, $P_3'(A) = 3a_3A^2 + 2a_2A + a_1$ so that $P_3'(0) = a_1 < 0$.

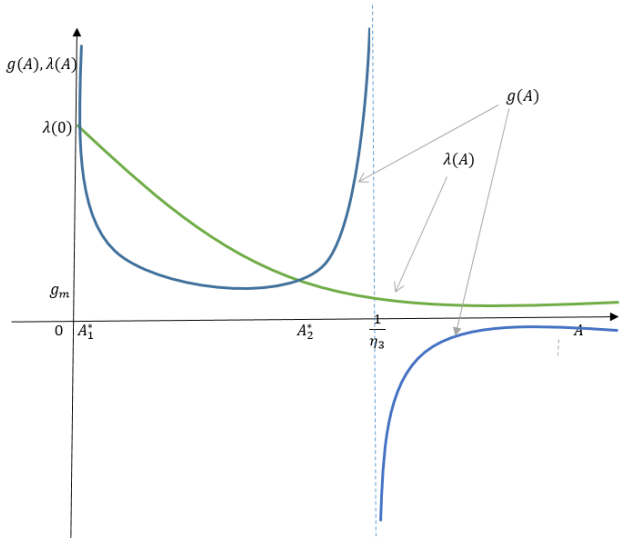

Figure B.9: An illustration of the proof of Theorem 2.3. Here, g is defined in (B.13) and λ is the Maynard Smith-Slatkin function with $n = 1$.

Next, we observe that no positive solution to $P_3(A^*) = 0$ can satisfy $A^* > \frac{1}{\eta_3}$. Suppose, for a contradiction, that $P_3(A) = 0$ has a positive solution $A^* > \frac{1}{\eta_3}$. Then $A^* = \frac{\omega}{\eta_3}$ for some $\omega > 1$ and $P_3\left(\frac{\omega}{\eta_3}\right) = 0$. Then

$$P_3(A^*) = P_3\left(\frac{\omega}{\eta_3}\right) = \frac{b\eta_3^2\lambda_0(\omega-1)\omega + (\alpha_3\eta_3 + \alpha_4\omega)\left(\beta_2\eta_3^2 + c\left(\eta_1+\eta_2\right)\omega^2 + \eta_3\omega\right)}{\eta_3^3} > 0,$$

contradicting the fact that A^* is a root of $P_3(A)$.

To complete the proof, let us denote

$$\Psi_{\lambda_0}(A^*) := \lambda(L(\eta_1+\eta_2)R_H^*) = \frac{\lambda_0(A^*+\beta_2)}{L(A^*+\beta_2) + \sigma A^{*2}}.$$

Then we observe that the graphs of Ψ_{λ_0} for different values of λ_0 do not intersect with the graph for a higher λ_0 is above the graph with a smaller one. This shows that $A_-^*(b\lambda_0') < A_-^*(b\lambda_0'')$ and $A_+^*(b\lambda_0') < A_+^*(b\lambda_0'')$ for $\lambda_0' > \lambda_0''$. Indeed, the point $(A_-^*(b\lambda_0''), \Psi_{\lambda_0'}(A_-^*(b\lambda_0'')))$ is above the graph

of g and therefore the intercept of g and $\Psi_{\lambda_0'}$ satisfies $A_-^*(b\lambda_0') < A_-^*(b\lambda_0'')$. The other statement follows in the same way. Furthermore, let us fix a small positive $\bar{A}$ and consider $g(\bar{A})+h$, where $h > 0$ is a constant. There is $\bar{\lambda}_0$ satisfying

$$\frac{\bar{\lambda}_0(\bar{A}+\beta_2)}{L(\bar{A}+\beta_2)+\sigma\bar{A}} = g(\bar{A}) + h,$$

and the point $(\bar{A}, \Psi_{\bar{\lambda}_0}(\bar{A}))$ is above the graph of g and thus $A_-^*(\bar{\lambda}_0) < \bar{A}$. This proves the first formula in (32). The other follows in the same way. □

An illustration of this proof is shown in Figure B.9. We can see that the tangency condition, $\lambda'(A^*) = g'(A^*)$, is satisfied when we have a single solution A^*.

Appendix B.11. Proof of Theorem 2.4

Combining the equations in (30) with the logistic form of λ gives

$$\lambda\left(LR_H^*(\eta_1+\eta_2)\right) = \lambda_0 b\frac{A^*+\beta_2-\sigma A^{*2}}{A^*+\beta_2} =: \Psi(A^*) = \frac{(\alpha_3+\alpha_4 A^*)(A^*+\beta_2)}{A^*(1-\eta_3 A^*)} =: \hat{g}(A^*). \quad \text{(B.23)}$$

We have

$$\Psi'(A^*) = -\lambda_0 b\frac{\sigma A^{*2}+2\sigma\beta_2 A^*}{(A^*+\beta_2)^2} < 0, \quad \Psi''(A^*) = -\lambda_0 b\frac{2\sigma\beta_2}{(A^*+\beta_2)^3} < 0$$

so, Ψ is decreasing and concave on $[0,\infty)$. Since $\hat{g}$ is a scalar multiple of g, it has the same properties and hence $\Psi''-\hat{g}'' < 0$ on $(0,\eta_3^{-1})$, which means that the function $\psi(A^*)-\hat{g}(A^*)$ is strictly concave and hence the equation $\psi(A^*)-\hat{g}(A^*)=0$ has two, one or no solutions. As before, we write $\Psi_{\lambda_0 b}$ to emphasize the dependence of Ψ on $\lambda_0 b$. Since the graphs of $\Psi_{\lambda_0 b}$ for different values of $\lambda_0 b$ do not intersect, and the graph with a smaller value is below the graph with a bigger one, we see that there exists a unique threshold value $\lambda_0^* b^*$, such that there are no solutions for $\lambda_0 b < \lambda_0^* b^*$, exactly one solution for $\lambda_0 b = \lambda_0^* b^*$ and two solutions for $\lambda_0 b > \lambda_0^* b^*$, as illustrated in Fig. B.10. The last part of the proof is done as for Theorem 2.3. First, A_+ is the single positive root of $\Psi_{\lambda_0 b}$, independent of $\lambda_0 b$. Thus, we always have $A_+(\lambda_0 b) < \min\{A_+, \eta_3^{-1}\}$ and, since $\lim_{\lambda_0 b\to\infty}\Psi_{\lambda_0 b}(\bar{A}) = \infty$ for any $\bar{A} < \min\{A_+, \eta_3^{-1}\}$, we can proceed as before. □

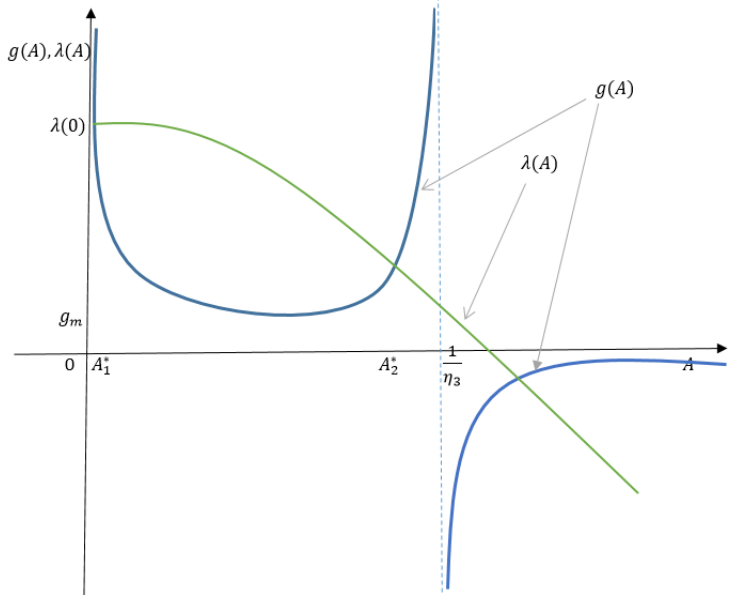

Figure B.10: An illustration of the proof of Theorem 2.4. A sketch of the graph of $\lambda\left(L\sigma\frac{A^2}{A+\beta_2}\right) = g(A)$, with g defined in (B.13) and λ the logistic function (16).

Appendix B.12. Proof of Theorem 2.5

The stability of the trivial steady states can be determined by observing the signs of the eigenvalues of the Jacobian matrix for system (26) evaluated at the trivial steady state $\mathbf{0}^* = (0,0,0,0,0,0,0,0)$. We have

$$J(\mathbf{0}^*) = \begin{pmatrix} -\alpha_3 & 0 & 0 & 0 & 0 & 0 & \alpha_1\lambda_0 & \alpha_2\lambda_0 \\ \beta_1 & -\beta_1 & 0 & 0 & 0 & 0 & 0 & 0 \\ 1 & 0 & -\beta_2 & 0 & 0 & 0 & 0 & 0 \\ 0 & 0 & 0 & -\beta_3 & 0 & 0 & \delta_1 & \delta_2 \\ 0 & 0 & 0 & \rho_1 & -\rho_1 & 0 & 0 & 0 \\ 0 & 0 & 0 & \rho_2 & 0 & -\rho_2 & 0 & 0 \\ 0 & 0 & 0 & 0 & 1 & 0 & -1 & 0 \\ 0 & 0 & 0 & 0 & 0 & \rho_3 & 0 & -\rho_3 \end{pmatrix}. \tag{B.24}$$

The characteristic polynomial of (B.24) is given by

$$|J(\mathbf{0}^*) - \zeta I| = (-\alpha_3 - \zeta)\,(-\beta_1 - \zeta)\,(-\beta_2 - \zeta)\,P_5(\zeta), \tag{B.25}$$

where $P_5(\zeta)$ is as defined in (34). The results follow since α_3, β_1 and β_2 are real and positive. □

Appendix B.13. Proof of Proposition 2.2

Writing the Jacobi matrix of (12) with the original parameters at the trivial equilibrium, we find from the Gershgorin theorem, [21], applied to the columns of the matrix, that the spectrum of this matrix is contained in the union of circles with centres at $-(\gamma+\mu_{A1}), -(\kappa+\mu_B), -(\tau_H H+\mu_{Q_H}), -(\tau_V V+\mu_{Q_V}), -(a_H+\mu_{R_H})$ and $-(a_V+\mu_{R_V})$ with radii, respectively, $(1-\theta)\gamma\xi+\theta\gamma\xi = \gamma\xi, \kappa\left(\frac{H}{H+\varsigma V}\right)+\kappa\left(\frac{\varsigma V}{H+\varsigma V}\right) = \kappa, p\tau_H H, q\tau_V V, a_H+\lambda_0 a_H$ and $a_V+\lambda_0 a_V$. Since $0 \le p, q \le 1$, we find that (35) imply that the spectrum is contained in the left half-plane of $\mathbb{C}$, yielding the asymptotic stability of the trivial equilibrium. □

Appendix B.14. Proof of Corollary 2.3

When $\rho_1 = \rho_2$, $\rho_3 = 1$, the polynomial P_5 defined in (34) reduces to

$$(\zeta+1)\,(\zeta+\rho_1)\left(-\beta_3(\zeta+1)\,(\zeta+\rho_1)+\rho_1\,(\delta_1+\delta_2-\zeta(\zeta+1))-\zeta^2(\zeta+1)\right). \tag{B.26}$$

Now, $(-\beta_3(\zeta+1)\,(\zeta+\rho_1)+\rho_1\,(\delta_1+\delta_2-\zeta(\zeta+1))-\zeta^2(\zeta+1)) = 0$ if and only if

$$P_3(\zeta) = \zeta^3 + p_2\zeta^2 + p_1\zeta + p_0 = 0, \tag{B.27}$$

where

$$p_0 = \rho_1\,(\beta_3-\delta_1-\delta_2), \quad p_1 = \beta_3\,(\rho_1+1)+\rho_1, \quad p_2 = \beta_3+\rho_1+1. \tag{B.28}$$

We then conclude stability using the Routh-Hurwitz conditions since $p_1p_2 - p_0 = \beta_3^2\,(\rho_1+1) + \beta_3\,(\rho_1+1)^2 + \rho_1\,(\delta_1+\delta_2+\rho_1+1) > 0$. □

Appendix B.15. Proof of Theorem 4.1

The eigenvalues of the Jacobian of (41) evaluated at the trivial steady state are roots of the polynomial

$$\hat{P}_6(\zeta) = (\alpha_3+\zeta)\,(\beta_1+\zeta)\,(\beta_2+\zeta)\,\hat{P}_3(\zeta), \tag{B.29}$$

$$\hat{P}_3(\zeta) = \zeta^3 + \hat{a}_2\zeta^2 + \hat{a}_1\zeta + \hat{a}_0, \tag{B.30}$$

where

$$\hat{a}_0 = \rho_1 (\beta_3 - \delta_1), \quad \hat{a}_1 = \beta_3 (\rho_1 + 1) + \rho_1, \quad \hat{a}_2 = \beta_3 + \rho_1 + 1. \tag{B.31}$$

Since $\beta_3 < \delta_1$, $\hat{a}_0 > 0$, $\hat{a}_1 > 0$, $\hat{a}_3 > 0$ and $\hat{a}_1\hat{a}_2 - \hat{a}_0 = \beta_3^2(\rho_1 + 1) + \beta_3(\rho_1 + 1)^2 + \rho_1(\delta_1 + \rho_1 + 1) > 0$, the results then follow from the Routh-Hurwitz stability criteria. □

Appendix B.16. Proof of Theorem 4.2

The steady states of (44) are given by $Q_H^* = B^* = R_H^*$, $R_H^* = \frac{A^*}{\beta_3 - \delta_1}$, where A^* is a non-negative solution of the equation

$$Ah(A) = 0, \quad h(A) = \frac{\alpha_1}{\beta_3 - \delta_1}\lambda\left(\frac{\eta_1 LA}{\beta_3 - \delta_1}\right)(1 - A) - (\alpha_3 + \alpha_4 A). \tag{B.32}$$

1. From (B.32), $A^* = 0$ is always a solution leading to the trivial steady state solution where $A^* = B^* = Q_H^* = R_H^* = 0$.
2. Notice that if λ is decreasing, then h is a strictly decreasing on $[0, 1]$. It is then easy to see that $h(0) = \alpha_3(\hat{\mathcal{B}}_H - 1)$ and $h(1) < 0$. Since h is continuous and strictly decreasing, the equation $h(A) = 0$ can only have a solution if $h(0) = \alpha_3(\hat{\mathcal{B}}_H - 1) > 0$, i.e., $\hat{\mathcal{B}}_H > 1$ and this solution is unique.
3. The Jacobi matrix of (47) evaluated at the trivial steady state is given by

$$J(\mathbf{0}) = \begin{pmatrix} -\alpha_3 & 0 & 0 & \alpha_1\lambda(0) \\ 1 & -\beta_3 & 0 & \delta_1 \\ 0 & \rho_1 & -\rho_1 & 0 \\ 0 & 0 & 1 & -1 \end{pmatrix}. \tag{B.33}$$

The characteristic polynomial of $J(\mathbf{0})$ is given by

$$\begin{aligned} P_4(\zeta) &= \zeta^4 + a_3\zeta^3 + a_2\zeta^2 + a_1\zeta + a_0, \\ a_0 &= \rho_1\alpha_3(\beta_3 - \delta_1)(1 - \hat{\mathcal{B}}_H), \quad a_1 = \alpha_3(\beta_3(\rho_1 + 1) + \rho_1) + \rho_1(\beta_3 - \delta_1) > 0, \\ a_2 &= \alpha_3(\beta_3 + \rho_1 + 1) + \beta_3(\rho_1 + 1) + \rho_1 > 0, \quad a_3 = \alpha_3 + \beta_3 + \rho_1 + 1 > 0. \end{aligned} \tag{B.34}$$

We notice that $a_0 > 0$ when $\hat{\mathcal{B}}_H < 1$. Some algebra shows us that $a_1a_2a_3 - a_1^2 - a_0a_3^2 > 0$, giving the stability of the trivial steady state whenever $\hat{\mathcal{B}}_H < 1$. Furthermore, examining the sequence of coefficients of the characteristic polynomial, $\{1, a_3, a_2, a_1, a_0\}$, we can notice that as $\hat{\mathcal{B}}_H$ increases from zero, there is no sign change in the sequence of coefficients whenever $\hat{\mathcal{B}}_H < 1$, and that as $\hat{\mathcal{B}}_H$ increases further to values of $\hat{\mathcal{B}}_H > 1$, a_0 becomes negative, hence, there is one sign change in the sequence of coefficients indicating the presence of one positive real eigenvalue. Thus, the trivial equilibrium loses stability.

4. Using similar analytical techniques as in [18, 32], we can establish that there is a range of system parameters for which the non-trivial steady state is stable whenever it exists and can be driven to instability via Hopf bifurcation.

□

References

[1] T. J. Alberg, A. Alampounti, and M. Georgiades. The Conversation. `https://bit.ly/mosquito-mating-sounds`, 2024. Accessed: 2024-09-10.

[2] W. C. Allee and E. S. Bowen. Studies in animal aggregations: Mass protection against colloidal silver among goldfishes. *Journal of Experimental Zoology*, 61(2):185–207, 1932.

[3] R. Anguelov, C. Dufourd, and Y. Dumont. Mathematical model for pest-insect control using mating disruption and trapping. *Applied Mathematical Modelling*, 52:437–457, 2017.

[4] R. Anguelov, Y. Dumont, and J. Lubuma. Mathematical modeling of sterile insect technology for control of anopheles mosquito. *Computers and Mathematics with Applications*, 64(3):374–389, 2012.

[5] R. Anguelov, Y. Dumont, and J. Lubuma. Mathematical modeling of sterile insect technology for control of anopheles mosquito. *Computers & Mathematics with Applications*, 64(3):374–389, 2012.

[6] J. Banasiak. *Introduction to Mathematical Methods in Population Theory*. Springer Verlag, Cham, 2024.

[7] J. Banasiak, B. M. Ghakanyuy, and G. A. Ngwa. A vector allee effect in mosquito dynamics. *Discrete and Continuous Dynamical Systems - Series B*, 30 (11):4162–4184, 2024.

[8] A. Bomblies, J. C. Dushoff, and M. A. Duchemin. Environmental and hydrological controls on malaria transmission. *Journal of Hydrology*, 365:175–191, 2008.

[9] J. D. Charlwood and M. D. R. Jones. Mating behaviour in the mosquito *Anopheles gambiae s. l.* i. Close range and contact behaviour. *Physiological Entomology*, 4(2):111–120, 1979.

[10] J. D. Charlwood, R. Thompson, and H. Madsen. Observations on the swarming and mating behaviour of *Anopheles funestus* from southern Mozambique. *Malaria Journal*, 2(2):`http://bit.ly/anopheles--funestus`, 2003.

[11] L. M. Childs, F. Y. Cai, E. G. Kakani, S. N. Mitchell, D. Paton, P. Gabrieli, C. O. Buckee, and F. Catteruccia. Disrupting mosquito reproduction and parasite development for malaria control. *PLoS Pathogens*, 12(12):e1006060, 2016.

[12] N. Chitnis, J. M. Cushing, and J. M. Hyman. Bifurcation analysis of a mathematical model for malaria transmission. *SIAM Journal on Applied Mathematics*, 67(1):24–45, 2008.

[13] N. Chitnis, T. Smith, and R. Steketee. A mathematical model for the dynamics of malaria in mosquitoes feeding on a heterogeneous host population. *Journal of Biological Dynamics*, 2(3):259–285, 2008.

[14] A. N. Clements. *The biology of mosquitoes. Volume 1: development, nutrition and reproduction.* Chapman & Hall, London, 1992.

[15] X. Fauvergue. A review of mate-finding Allee effects in insects: from individual behavior to population management. *Entomologia Experimentalis et Applicata*, 146(1):79–92, 2013.

[16] D. A. Focks, E. Daniels, D. G. Haile, and J. E. Keesling. A simulation model of the epidemiology of urban dengue fever. *Journal of Medical Entomology*, 30:1003–1017, 1993.

[17] Centers for Disease Control and Prevention. Mosquito life cycle, 2023. Accessed: 2025-02-05.

[18] B. M. Ghakanyuy, M. I. Teboh-Ewungkem, K. A. Schneider, and G. A. Ngwa. Investigating the impact of multiple feeding attempts on mosquito dynamics via mathematical models. *Mathematical Biosciences*, 350:108832, 2022.

[19] D. Goindin, C. Delannay, C. Ramdini, J. Gustave, and F. Fouque. Parity and longevity of aedes aegypti according to temperatures in controlled conditions and consequences on dengue transmission risks. *PloS One*, 10(8):e0135489, 2015.

[20] L. Gomulski. Polyandry in nulliparous *Anopheles gambiae* mosquitoes (diptera: Culicidae). *Bulletin of Entomological Research*, 80(4):393–396, 1990.

[21] A. Hetmaniok, M. Pleszczyński, M. Różański, D. Słota, T. Trawiński, R. Witula, and A. Wróbel. *Zagadnienia lokalizacyjne wartości własnych macierzy w powiązaniu z twierdzeniem Gerszgorina (Location problems of the matrix eigenvalues in connection with the Gerschgorin Theorem)*. Wydawnictwo Politechniki Śląskiej, Gliwice, 2018.

[22] G. B. Craig Jr. Mosquito: female monogamy induced by a male accessory gland substance. *Science*, 156(781):1499–1501, 1967.

[23] J. M. Klowden. Sexual receptivity in *Anopheles gambiae* mosquitoes: absence of control by male accessory gland substances. *Journal of Insect Physiology*, 47(7):661–166, 2001.

[24] R. S. Lees, J. R. L. Gilles, J. Hendrichs, M. J. B. Vreysen, and K. Bourtzis. Back to the future: the sterile insect technique against mosquito disease vectors. *Current Opinion in Insect Science*, 10:156–162, 2015.

[25] J. Li. Malaria model with stage-structured mosquitoes. *Mathematical Biosciences and Engineering*, 8(3):753–768, 2011.

[26] J. Li. Discrete-time models with mosquitoes carrying genetically-modified bacteria. *Mathematical Biosciences*, 240(1):35–44, 2012.

[27] J. Li, L. Cai, and Y. Li. Stage-structured wild and sterile mosquito population models and their dynamics. *Journal of Biological Dynamics*, 11:79–101, 2017.

[28] P. L. Lounibos and R. L. Escher. Sex ratios of mosquitoes from long-term census of florida tree holes. *Journal of the American Mosquito Control Association*, 24(1):11–15, 2008.

[29] A. M. Lutambi, M. A. Penny, N. Chitnis, and T. Smith. Mathematical modelling of mosquito dispersal in a heterogeneous patchy environment. *Mathematical Biosciences*, 241(2):198–216, 2013.

[30] J. D. Murray. *Mathematical biology. II*, volume 18 of *Interdisciplinary Applied Mathematics*. Springer-Verlag, New York, third edition, 2003.

[31] C. N. Ngonghala, M. I. Teboh-Ewungkem, and G. A. Ngwa. Observance of period-doubling bifurcation and chaos in an autonomous ode model for malaria with vector demography. *Theoretical Ecology*, 9(3):337–351, 2016.

[32] G. A. Ngwa. On the population dynamics of the malaria vector. *Bulletin of Mathematical Biology*, 68(8):2161–2189, 2006.

[33] G. A. Ngwa, A. M. Niger, and A. B. Gumel. Mathematical assessment of the role of non-linear birth and maturation delay in the population dynamics of the malaria vector. *Applied Mathematics and Computation*, 217(7):3286–3313, 2010.

[34] G. A. Ngwa, M. I. Teboh-Ewungkem, Y. Dumont, R. Ouifki, and J. Banasiak. On a three-stage structured model for the dynamics of malaria transmission with human treatment, adult vector demographics and one aquatic stage. *Journal of Theoretical Biology*, 481:202–222, 2019.

[35] G. A. Ngwa, T. T. Wankah, M. Y. Fomboh-Nforba, C. N. Ngonghala, and M. I. Teboh-Ewungkem. On a reproductive stage-structured model for the population dynamics of the malaria vector. *Bulletin of Mathematical Biology*, 76:2476–2516, 2014.

[36] E. C. Pielou. *Mathematical ecology*. Wiley-Interscience [John Wiley & Sons], New York-London-Sydney, second edition, 1977.

[37] O. Romoli, J. Serrato-Salas, C. Gapp, Y. Epelboin, P. F. Ivern, F. Barras, and M. Gendrin. Nutritional sex-specificity on bacterial metabolites during mosquito (aedes aegypti) development leads to adult sex-ratio distortion. *Biology Communications*, 7(1):123–135, 2024.

[38] J. Klaška. On cubic polynomials with a given discriminant. *Mathematics for Applications (Brno)*, 10(2):103–113, 2021.

[39] H. L. Smith and P. Waltman. *The theory of the chemostat: dynamics of microbial competition*, volume 13. Cambridge University Press, 1995.

[40] K. Snyder, B. Kohler, and L. F. Gordillo. Mass action in two-sex population models: encounters, mating encounters and the associated numerical correction. *Letters in Biomathematics*, 4(1):101–111, 2017.

[41] M. Strugarek, H. Bossin, and Y. Dumont. On the use of the sterile insect release technique to reduce or eliminate mosquito populations. *Applied Mathematical Modelling*, 68:443–470, 2019.

[42] L. M. Styer, J. R. Carey, J.-L. Wang, and T. W. Scott. Mosquitoes do senesce: departure from the paradigm of constant mortality. *The American journal of tropical medicine and hygiene*, 76(1):111, 2007.

[43] W. Takken, C. Constantini, G. Dolo, A. Hassanali, N. Sagnon, and E. Osir. Mosquito mating behaviour. In *Bridging laboratory and field research for genetic control of disease vectors*, volume 11, pages 183–188. Springer Verlag, 2006.

[44] Vector Disease Control International. Mosquito biology 101: Life cycle. `<ahref="https://www.vdci.net/mosquito-biology-101-life-cycle/">https://www.vdci.net/mosquito-biology-101-life-cycle/</a>`, 2024. Accessed: November 23, 2024.

[45] C. Villarreal, G. Fuentes-Maldonado, MH Rodriguez, and B. Yuval. Low rates of multiple fertilization in parous anopheles albimanus. *Journal of the American Mosquito Control Association*, 10(1):67–69, 1994.

[46] M. T. White, G. F. Killeen, N. J. Govella, and F. O. Okumu. Mathematical modelling of mosquito dispersal in a heterogeneous environment. *PLoS Computational Biology*, 7(6), 2011.

[47] W. A. Woldegerima, M. I. Teboh-Ewungkem, and G. A. Ngwa. Assessing the impact of the rate of recruitment of red blood cells in the immuno-pathogenesis of the within-human-host *Plasmodium falciparum* parasite dynamics. *Bulletin of Mathematical Biology*, 81:4564–4619, 2019.

[48] S. Xue, M. Li, J. Ma, and J. Li. Sex-structured wild and sterile mosquito population models with different release strategies. *Mathematical Biosciences and Engineering*, 16(3):1313–1333, 2019.

[49] B. Yuval and G. N. Fritz. Multiple mating in female mosquitoes: evidence from a field population of anopheles freeborni (diptera: Culicidae). *Bulletin of Entomological Research*, 84(01):137–139, 1994.